Detlef Quadfasel
Institut für Meereskunde
Zentrum für Marine und Atmosphärische Wissenschaften
Universität Hamburg
Bundesstr. 53
D-20146 Hamburg

Tel.: +49 40 42838 5756
Fax: +49 40 42838 7477
e-mail: detlef.quadfasel@zmaw.de

Cruise Report
RRS Discovery Cruise D311

Reykjavik - Reykjavik - Reykjavik
8. September – 20.September – 6. October 2006
Chief Scientist: Detlef Quadfasel
Captain: Peter C. Sarjeant

Technical Report 1-06

On citing this report in a bibliography, the reference should be followed by the words *unpublished manuscript.*

The scientific party of RRS DISCOVERY cruise D311 leg. The photo was takes after completion of the leg in the port of Reykjavik.

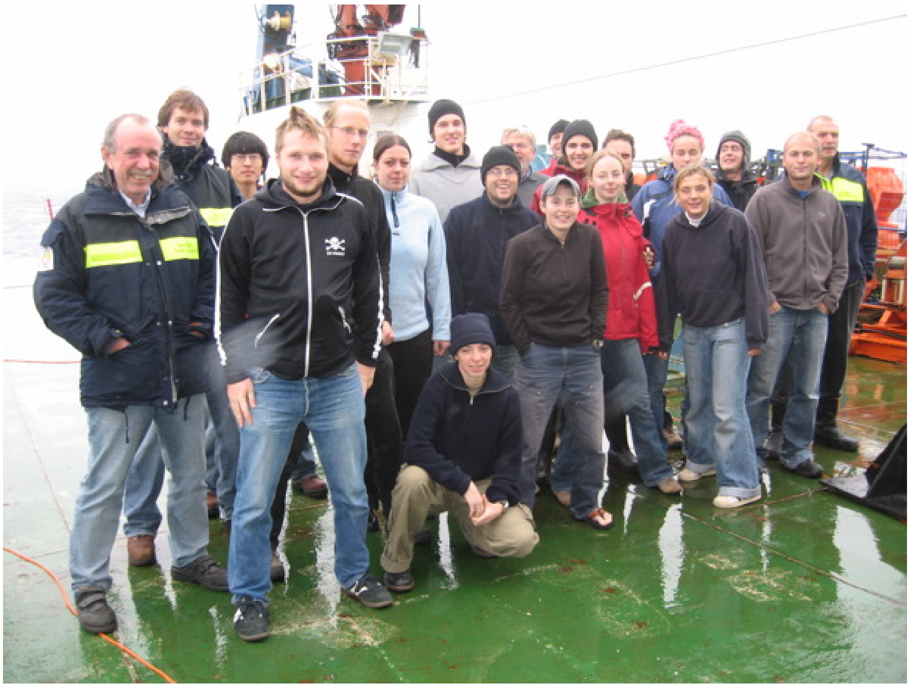

The scientific party of RRS DISCOVERY cruise D311 leg 2. The photo was takes on Discovery's aft deck in wind force 7.

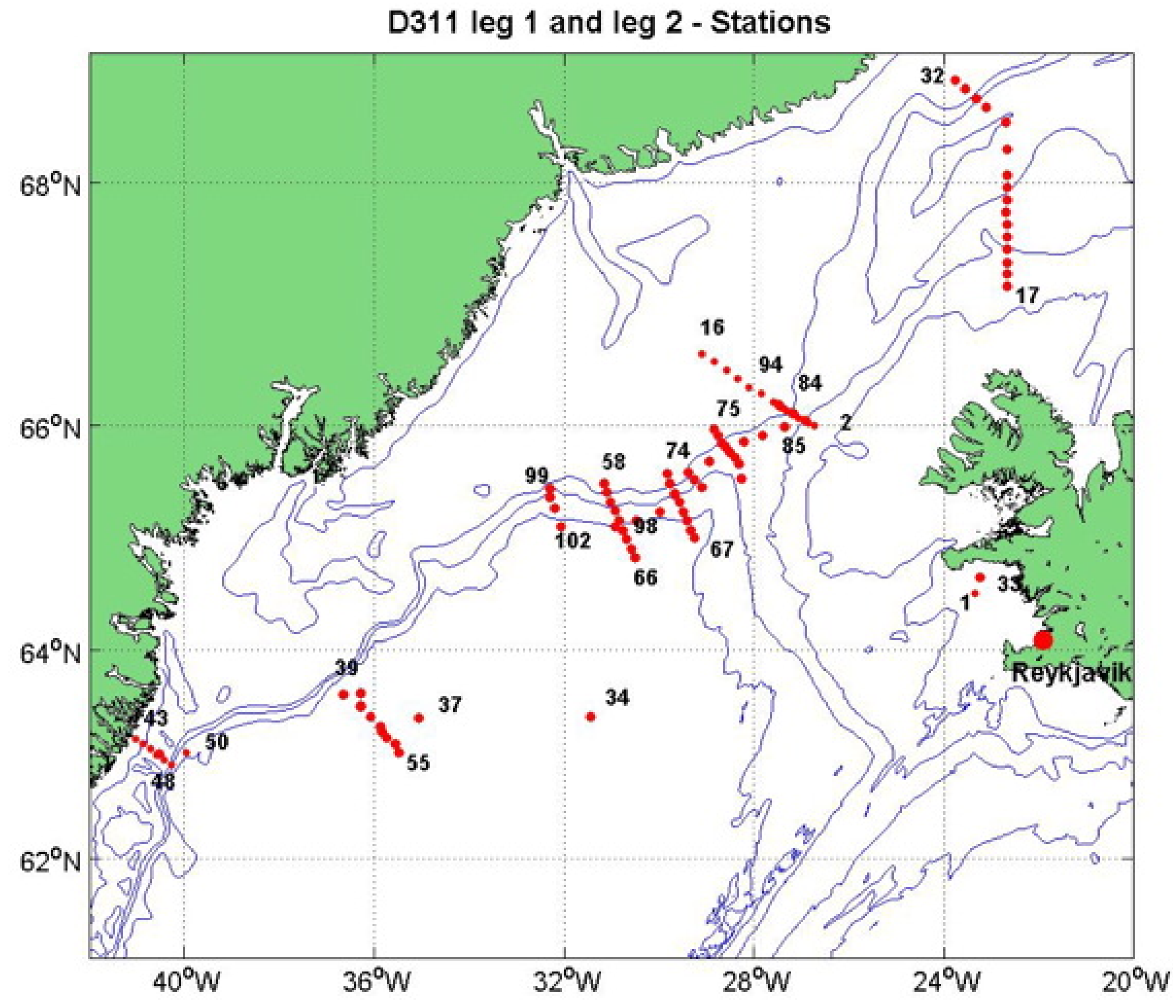

Positions of hydrographic and mooring stations occupied during RRS DISCOVERY cruise D311

1. Objectives

RRS DISCOVERY cruise D311 was carried out by the Institut für Meereskunde at the Centre for Marine and Atmospheric Sciences of the University of Hamburg (IfM-ZMAW), with participation of the Centre for Environment, Fisheries and Aquaculture Science (CEFAS), the Finnish Institute of Marine Research (FIMR), the Woods Hole Oceanographic Institution (WHOI), the Lamont Doherty Geological Observatory (LDEO), the University of Gent (UGent) and the University of East Anglia (UEA).

The objective of the Discovery cruise D311 was to study different aspects of the Denmark Strait overflow. The first part of the cruise concentrated on examining the water masses at the sill and the upstream conditions in the East Greenland Current and in the Iceland Sea. Two pathways of overflow water were discovered north of Denmark Strait. One flows along the Greenland continental slope and involves waters from the Arctic Ocean, Fram Strait and the Greenland Sea. The other runs on the north-western Iceland shelf and apparently carries the densest overflow water. The origin of this water mass is not yet determined. Does it derive from the Iceland Sea or does it come from farther north? To resolve this question the water mass characteristics in the East Greenland Current and in the Iceland Sea was examined by CTD observations and water sampling involving CFCs, H3, He3, O2, O18. In addition attempts to recover moorings with an ROV were made. The first leg ended in Reykjavik, where exchange of scientific personnel took place.

After the exchange Discovery continued to the Greenland slope, where the VEINS and ASOF CTD sections were taken and the mooring array at Angmassalik recovered and redeployed. The purpose of these sections south of the sill in Denmark Strait was to study the evolution, strength and variability of the overflow plume – how the different water masses from north of the sill mix on their way to the south and how much and by what mechanisms ambient water is entrained into the overflow plume. To study these processes the CTD observations and the water sampling were complemented by turbulence measurements using a freefalling CTD and current meter probe. In addition, an autonomous glider was deployed.

Attending this 4-week cruise, students from the University of Hamburg got the opportunity to practice a scientist's work on board. The students assisted CTD measurements, took water samples and started to process the data obtained. Additionally an oceanographic seminar took place every day. A summary of the students work during the cruise can be found at
http://www.ifm.uni-hamburg.de/~wwwro/quadfasel/teaching/ss2006_discovery/cruise_site/D311_website/index.html

2. Narrative

6. September 2006
Position: Port of Reykjavik

With some delay the containers arrived during the afternoon and were subsequently unloaded. Securing the ROV container on the aft deck required some welding work which took until early evening.

7. September 2006
Position: Port of Reykjavik

Preparation of the instrumentation continued. All went well, except the tests with the ROV failed. Because of this sailing of the vessel was postponed until noon the next day. The Hamburg students arrived during the afternoon.

8. September 2006
Noon Position: Port of Reykjavik

After breakfast the captain gave a safety briefing for the scientific crew. Several shortcuts in the ROV power supply and data links demanded further repair work. It was decided to postpone sailing to 10 a.m. the next day. During the afternoon the students received an introduction into instrument handling and sampling procedures.

9. September 2006
Noon Position: 64°19.2' N 22°25.6' W
Wind direction: 270° / Wind speed: 20 knots / Air temperature: 9.5°C

After an emergency consultation with the Gent Laboratory it was decided to leave the ROV on board, even though it did not work yet, and to attempt the repair during the cruise. Discovery sailed at 10:00 h. About an hour later the first students became seasick. During the afternoon a CTD test station was run successfully. At 4 p.m. we had an Emergency and lifeboat muster.

10. September 2006
Noon Position: 66°07.24' North / 27°16.19' West
Wind direction: 190° / Wind speed: 18 knots / Air temperature: 7.5°C

Scientific watches started with the morning shift. The CTD section along the sill of Denmark Strait started at 9 a.m. Salinity signals were very noisy and as cleaning of the sensors did not help the pump and conductivity sensor were exchanged. At 1 p.m. an attempt was made to recover the ADCP mooring in Denmark Strait, but no acoustic response was received from the releasers. A release signal was sent anyway, but the mooring did not surface and after an hour we went back to the CTD positions and resumed the hydrographic section.

11. September 2006
Noon Position: 66°10.61' North / 27°29.02 West
Wind direction: 210° / Wind speed: 20 knots / Air temperature: 3.3°C

On station 6 the pump of the CTD broke and had to be replaced. The sensor package was moved from the fin to the interior of the rosette, which reduced the noise on the traces significantly. During the day the weather improved and the Denmark Strait section was continued. A first sighting of whales caused excitement with the students. During the night colourful northern lights showed up at the horizon.

12. September 2006
Noon Position: 66°51.987' North / 26°47.062' West
Wind direction: 070° / Wind speed: 18 knots / Air temperature: 3.3°C

After 16 stations the Denmark Strait section was completed at 9 a.m. Because of a gale warning we decided to steam north to run a CTD section along 21° 40' W, from the shelf break of Iceland to the north. In the evening we had a little party celebrating the crossing of the Arctic circle the night before. The first station (No. 17) of the second section was reached at 9 p.m.

13. September 2006
Noon Position: 67°32.377 North / 22°26.236 West
Wind direction: 070° / Wind speed: 40 knots / Air temperature: 5.3°C

Increasing winds forced us to stop work on station 19 and the ship had to stay hove to.

The students started with working up the CTD data and were assigned small scientific projects.

14. September 2006
Noon Postion: 67°26.8' North / 22°45.9' West
Wind direction: 055° / Wind speed: 35-40 knots / Air temperature: 5.0°C

The weather did not improve and the ship stayed hove to. The captain started a series of navigation courses for the students, which was extremely well received.

15. September 2006
Noon Position: 67°39.52' North / 22°27.612' West
Wind direction: 045° / Wind speed: 40 knots / Air temperature: 2.6°C

No change of weather. The day was spent with student seminars and a test of their knowledge on security procedures. Because of cheating Koen was disqualified; Alison won by scoring 21 points. Her prize was a Discovery mug.

16. September 2006
Noon Position: 67°51.667' North / 22°14. 541' West
Wind direction: 020° / Wind speed: 20-25 knots / Air temperature: 2.8°C

The weather improved slightly and by 10:30 a-m. we sailed back to position 20 on the CTD section. Work resumed at 3 p.m.

17. September 2006
Noon Postion: 68°35.834' North / 22°06.447' West
Wind direction: 045° / Wind speed: 25 knots / Air temperature: 0.6°C

During the night winds were very calm and good progress was made along the section. However, since the forecast was bad again, some stations were skipped in order to complete the section across the East Greenland continental slope The weather became worse again in the afternoon but we were able to work until 9 p.m. by which time wind reached 9 Bft again. The students enjoyed a beautiful sunset the Greenland glaciers before they had a theory lesson given by Professor Zahel. Due to the strong winds and swell from the north-east it was decided to change the mid-cruise port call from Akureyri to Reykjavik and the agent and scientists for the next leg were informed accordingly.

18. September 2006
Noon Position: 66°31.4' North / 25°16.3' West
Wind direction: 055° / Wind speed: 45 knots / Air temperature: 3.6°C

Steaming towards Reykjavik with 10m swell from aft. This was an impressive roler coater ride under a blue sky. The students were busy working up data preparing the project presentations. In the evening the Belgian colleagues gave a presentation about their ROV, which by then worked properly, at least in the hangar.

19. September 2006
Noon Position: 64°40.0' North / 23°13.7' West
Wind direction: 070° / Wind speed: 18 knots / Air temperature: 11.8°C

We were once again near the Icelandic coast with a beautiful view over and in shelter of snow covered mountains. Jules Verne used one of those volcanoes as an entrance to the middle of the earth. The ROV was launched in a water depth of 70 m and provided pictures of the shelf bottom. The instrument worked well – finally – but unfortunately too late for the planned mooring recovery work. Discovery went alongside in Reykjavik harbour at 8 p.m. and the first leg of cruise D311 was finished. The evening saw the student's project presentations, which were followed by a little farewell party.

20. September 20/06
Noon position: Port of Reykjavik

The new scientific crew arrived at 10 a.m. and the "old" student-crew left at 1 p.m. for the airport. The ROV container was offloaded and the equipment for the microstructure probe was taken on board. Discovery sailed at 3 p.m., heading for the line of moorings to be recovered and re-deployed.

21. September 2006
Noon position: 63°44.6' North / 30°03.2' West
Wind direction: 045° / Wind speed: 20 knots / Air temperature: 8.4°C

At 4 p.m. a test of the Microstructure probe was attempted, but before going into the water some problems occurred with the winch system and the test was abandoned.

22. September 2006
Noon position: 63°20.2' North / 36°00.1' West
Wind direction: various / Wind speed: light airs / Air temperature: 7.5°C

Discovery reached the first mooring position at 6 a.m. but the release of the mooring failed. No response signal was detected. After several tries it was decided to move to the next mooring and by 6 p.m. all four remaining moorings along the Angmassalik line were recovered. We then sailed to the position of the shallow moorings on the East Greenland shelf.

23. September 2006
Noon position: 63°00.3' North / 40°33.2' West
Wind direction: 025° / Wind speed: 25 knots / Air temperature: 1.4°C

The bottom mounted ADCP mooring was successfully grappled at 9:30 a.m. and was on deck half an hour later. After an unsuccessful attempt to recover tube-mooring 21 we deployed its replacement by 4.30 p.m. A CTD section was then run across the shelf with the first station being only 3 miles off the Greenland coast. Unfortunately the weather was quite foggy so the tourist aspects of this section were not met to well. The section was then run offshore, out of the region where many ice berg were floating around.

24. September 2006
Noon position: 63° 01.1' North / 40° 34.5' West
Wind direction: 015° / Wind speed: 45-55 knots / Air temperature: 1.8°C

During the night the weather became increasingly stormy, so we had to stop our work after station 48 was completed at 4 a.m.. Discovery stayed hove to throughout the day and the time was spent with data analysis and student seminars.

25. September 2006
Noon position: 63° 01.1' North / 40° 29.3' West
Wind direction: 030° / Wind speed: 30 knots / Air temperature: 4.6°C

Winds ceased slightly during the night and we were able to reach the ADCP deployment position by 8:30 a.m. The ADCP with a ground line was successfully deployed by noon. After one more CTD station the WHOI glider was deployed during the afternoon and we steamed back to the Angmassalik array location.

26. September 2006
Noon position: 63° 30.8' North / 36° 24.9' West
Wind direction: 070° / Wind speed: 20 knots / Air temperature: 9.3°C

Except for the dense fog the weather conditions were perfect for the mooring deployments, which started at 9 a.m. with mooring F1/2 and finished with the fourth mooring UK2 at 6 p.m. Because of the fog no attempt was made to recover the Aqualab, but instead another Microstructure probe trial was made. Again there were problems with the winch and the test had to be abandoned. A second attempt to make contact with mooring G2 failed and a CTD section along the mooring line was started.

27. September 2006
Noon position: 63° 14.1' North / 35° 51.2' West
Wind direction: 040° / Wind speed: 30 knots / Air temperature: 8.4°C

Stephen Dye's birthday. With winds gusting to 45 knots work had to be abandoned by 1 a.m. To more CTD profiles were taken during the morning, when winds appeared to calm down, but by noon winds and waves had picked up again so that no more work was possible. Discovery sailed to the Aqualab position where acoustic contact was made, but due to the heavy swell we decided against releasing the mooring. Since the weather forecast for the region showed winds of 8 Bft. for the next two days, we decided to sail north towards Denmark Strait.

28. September 2006
Noon position: 63° 59,5' North / 34° 11.6' West
Wind direction: 045° / Wind speed: 50 knots / Air temperature: 5.3°C

It was stormy the whole day with wave heights of up to 9 meters. The ship's speed was just about 2 knots. The students spent the day in front of the computers, and were given a course in knot making by the bosun. Also the captain gave a course in navigation. In groups of three students we were allowed to go up and ask everything about the instruments on the bridge. Stephen Dye gave a presentation on 'Overflow and freshwater: ocean fluxes south of Denmark Strait'.

29. September 2006
Noon position: 64° 59.5' North / 31° 53.3' West
Wind direction: 030° / Wind speed: 35 knots / Air temperature: 4.8°C

During the day the swell ceased slightly allowing another test of the Microstructure probe. For the first time the instrument worked properly. During the night we continued with a CTD section across the overflow plume

30. September 2006
Noon position: 64°55,1' North / 30°35,3' West
Wind direction: 025°/ Wind speed: 18 knots / Air temperature: 5.6°C

The weather was good and the mood of the scientists was the same: the sun was shining, the sea was calm and we saw a lot of whales again. A pod of more than ten Pilot whales swam right beside the ship, spouting water. In the afternoon we discontinued the current CTD section because it had passed the overflow plume. We started a new section some 30 miles upstream, had a great sunset and fantastic northern lights later in the night. Unfortunately the slip rings in the Microstructure winch had been flooded with sea water and required some cleaning and repair.

1. October 20/06
Noon positon: 65° 46.0' North / 29° 20.0' West
Wind direction: various / Wind speed: light airs / Air temperature: 4.4°C

Perfect weather again. The CTD and Microstructure work went smooth and it was decided to drag for the mooring in Denmark Strait the next day, after finishing the hydrographic sections in the south.

2. October 2006
Noon position: 66° 07.2' North / 27° 16.5' West
Wind direction: 160° / Wind speed: 12 knots / Air temperature: 4.1°C

The final CTD station on the section ended at 5 a.m. and by 9 a.m. Discovery reached the mooring position on the Denmark Strait sill. Two attempts were made with 1600 m of wire out, but both of them were not successful. (It turned out later, that the mooring had broken off the anchor about 3 weeks earlier. It was found drifting and recovered by Faroese fishermen who delivered it back to the Faroese Oceanographic Institute). After lunch the students had the opportunity to visit the engine room. At 6 p.m. CTD work was taken up again.

3. October 2006
Noon position: 65°31.5' North / 29°15.7' West
Wind direction: 190° / Wind speed: 17 knots / Air temperature: 7.8°C

CTD work continued throughout the day, after completing the Denmark Strait section we ran along the bottom topography following the overflow plume downstream.

3. October 2006
Noon position: 65°16.9' North / 32°12.1' West
Wind direction: 010° / Wind speed: 20 knots / Air temperature: 3.9°C

We completed our last CTD measurement at 4 p.m. and Discovery set course to Reykjavik Harbour. Instrumentation was stored away, laboratories cleaned and the evening saw a great party, organized by Bert Rudels on the occasion of his birthday. We also held a photo competition that as won by Alison with her picture of a big wave.

5. October 2006
Noon position: 64°58.8' North / 32°12.1' West
Wind direction: 070° / Wind speed: 15 knots / Air temperature: 8.0°C

Continued cleaning and packing. Discovery was alongside at 8 p.m. and cruise D311 was finished.

6. October 2006
Noon position: Reykjavik Harbour

Demobilising, packing of the containers ashore. The scientific party disembarked at around noon.

3. Cruise participants

Scientific party:

Participants leg 1:

Detlef Quadfasel (Ch.Sc.)	IfM – ZMAW	quadfasel(at)ifm.zmaw.de
Andreas Welsch	IfM – ZMAW	welsch(at)ifm.zmaw.de
Norbert Verch	IfM – ZMAW	verch(at)ifm.zmaw.de
Wilfried Zahel	IfM – ZMAW	zahel(at)ifm.zmaw.de
Bert Rudels	FIMR	rudels(at)fimr.fi
Alison Criscitiello	LDEO	crisciti(at)ldeo.columbia.edu
Willem Versteeg	UGent	willem.versteeg(at)ugent.be
Jeroen Vercruysse	UGent	jeroenvercruysse(at)telenet.be
Koen De Rycker	UGent	koen.derycker(at)ugent.be

Meike Kühnel	student IfM
Gerrit Maschwitz	student IfM
Antje Müller-Michaelis	student IfM
Katharina Prenzel	student IfM
Nicole Rüther	student IfM
Anna Catrin Schmidt	student IfM
Anna Sellhorn Timm	student IfM
Rita Thönnes	student IfM
Moritz Wellner	student IfM
Max Wicklein	student IfM

Participants leg 2:

Detlef Quadfasel (Ch.Sc.)	IfM – ZMAW	quadfasel(at)ifm.zmaw.de
Andreas Welsch	IfM – ZMAW	welsch(at)ifm.zmaw.de
Norbert Verch	IfM – ZMAW	verch(at)ifm.zmaw.de
Gunnar Voet	IfM – ZMAW	voet(at)ifm.zmaw.de
Bert Rudels	FIMR	rudels(at)fimar.fi
Stephen Dye	CEFAS	s.r.dye(at)cefas.co.uk
Neil Needham	CEFAS	neil.needham(at)cefas.co.uk
Peter Winsor	WHOI	pwinsor(at)whoi.edu
Peter Sugimura	WHOI	psugimura(at)whoi.edu
Alison Criscitiello	LDEO	crisciti(at)ldeo.columbia.edu
Gareth Alan Lee	UEA	G.A.Lee(at)uea.ac.uk

Antje Müller-Michaelis	student IfM
Alexander Beitsch	student IfM
Simon Brinkrolf	student IfM
Nina Maaß	student IfM
Michaela Markovic	student IfM
Lucia Rau	student IfM
Theresa Reichelt	student IfM
Bente Tiedje	student IfM
Christian Zoller	student IfM

IfM-ZMAW: Institut für Meereskunde
Centre for Marine and Atmospheric Sciences
University of Hamburg
Bundesstr. 53
D-22529 Hamburg
Germany

CEFAS: Centre for Environment, Fishery and Aquaculture Sciences
Lowestoft Laboratory
Pakefield Road
Lowestoft Suffolk NR33 0HT
U.K.

UEA: School of Environmental Sciences
University of East Anglia
Norwich NR4 7TJ
U.K.

FIMR: Finnish Institute of Marine Research
P.O. Box 33
FIN-00931 Helsinki
Finland

WHOI: Woods Hole Oceanographic Institution
266 Woods Hole Road
Woods Hole, MA 02543-1050
U.S.A.

UGent: Renard Centre of Marine Geology
Department of Geology and Soil Science
Ghent University
Krijgslaan 281 s.8
B-9000 Gent
Belgium

LDEO: Lamont Doherty Earth Observatory
PO Box 1000
Palisades, NY 10964-8000
U.S.A.

UKORS technical staff:

Martin Bridger	TECH	UKORS
Darren Young	TECH	UKORS
John Wynar	TECH	UKORS

UKORS: Ocean Engineering Division
United Kingdom Ocean Research Services
Southampton Oceanographic Centre
European Way
Southampton SO14 3ZH
U.K.

Ship crew:

Peter C. Sarjeant	MASTER
Philip D. Gauld	C/O
Annalara P. Kirkaldi-Willis	2/O
Katie E. Rumbold	3/O
David S. Bendell	Cadet
Stephen A. Moss	C/E
Stephen J. Bell	2/E
Gary Slater	3/E
Anthony Healy	3/E
Dennis WJ Jakobaufderstroth	ETO
David R. Hartshorne	PCO
Michael J Drayton	CPOD
Michael Minnock	CPOS
Philip Allison	Seaman
Gerald Cooper	SG1A
Gary Crabb	SG1A
William M McGeown	Sm/Grade
Lee Stephens	S/Man 1A
Leslie J Hillier	MM1A
John Haughton	Chef
Stephen R Nagle	Chef
Darren A Caines	Asst Chef
Graham M Mingay	Stwd

5. Technical information

John Wynar

CTD system

A total of 88 CTD casts were completed on this cruise, the numbering of each cast being some-what unconventional. Each site occupied had a separate station number, and if a CTD was repeated it's cast number was incremented. The initial sensor configuration was as follows:

Sea-Bird 9*plus* underwater unit, s/n 09P-37898-0782
Sea-Bird 3 Premium temperature sensor, s/n 03P-4489 (Frequency 0)
Sea-Bird 4 conductivity sensor, s/n 04C-2407 (Frequency 1)
Digiquartz temperature compensated pressure sensor, s/n 94756 (Frequency 2)
Sea-Bird 3 Premium temperature sensor, s/n 03P-4490 (Frequency 3)
Sea-Bird 4 conductivity sensor, s/n 04C-2450 (Frequency 4)
Sea-Bird 43 dissolved oxygen sensor, s/n 43-0612 (V0)
Benthos PSA-916T 7Hz altimeter, s/n 1040 (V2)
Chelsea Aquatracka MKIII fluorometer, s/n 88-2360-108 (V3)
WETLabs Light Scattering sensor, s/n BBRTD-169 (V6)
Chelsea Alphatracka MKII transmissometer, s/n 04-4223-001 (V7)
Sea-Bird 11*plus* deck unit, s/n 11P-19817-0495

<u>Ancillary instruments & components:</u>

Sea-Bird 24-position Carousel, s/n 32-24680-0344
NOC/SBE 'Break-Out Box', s/n BO19107T
NOC 10KHz acoustic pinger, s/n B12
Sonardyne HF Deep Marker Beacon, s/n 215303-01
RDI WorkHorse Monitor 300KHz ADCP, s/n 1881 (Master: downward-looking)
RDI WorkHorse Monitor 300KHz ADCP, s/n 5414 (Slave: upward-looking)
NOC/RDI aluminium Workhorse battery pack, s/n WH001
14 x Ocean Test Equipment ES-10L water samplers, s/n 01 to 14 inc.

<u>User supplied instrument:</u>

SBE35RT temperature sensor, s/n: 43585-0028

CTD analysis & changes to configuration:

A) Prior to the station/cast 1/1, the Break-Out Box or BOB (s/n: BO19106) was replaced due to severe corrosion across the power and ground pins of the JT5/Aux3 bulkhead connector. It was exchanged with the titanium BOB (s/n: BO19107T).

B) Data spikes on the primary salinity display were observed on the first "shake-down" station 1/1, and the 11*plus* deck unit indicated that the primary pump was not operating occasionally on the downcast. Connectors on the instruments and the cables were cleaned and inspected, but the fault repeated and even deteriorated during the next cast, 2/1. The primary conductivity cell (s/n: 4C-2407) and it's cable was replaced (with s/n: 4C-2164) resulting in considerably fewer data spikes on the next cast, 2/a. The pump also operated normally for both the downcast and upcast. To attempt to remove the remaining data spikes, the primary temperature sensor (s/n: 3P-4489) was replaced (with s/n: 3P-4151). The following station, 3/1 produced fewer data spikes still, and all subsequent ones showed no further spikes.

C) During station 3/1 the altimeter display remained at 0 for the entire cast. Removing and cleaning connectors had no effect so the altimeter (s/n: 1040) was replaced with the spare Benthos unit (s/n: 1037). This again made no difference until the altimeter was re-selected in the Seasave software. It then began to display the correct in-air value of 98.5. It was speculated that the fault lay in the software and not hardware and that the altimeters would be exchanged at some convenient time to prove this. This happened prior to station 20/1 when the original Benthos altimeter was fitted. The altimeter display operated normally, hence the original unit (s/n: 1040) was left in place.

D) CTD cast 6/1 was abandoned due to a re-occurrence of severe data spiking. The replay indicated that the spiking began on the secondary channel before it affected the primary. Examination of the instrument revealed a broken connector on the secondary pump (s/n: 053965). The secondary instruments had been fitted to the CTD vane on a previous cruise, with the pump attached on the vane and slightly proud of it, nearest to the frame and close to a vertical frame member. This left the pump connector vulnerable to any lateral movement of the vane relative to the frame. Hence, the damage was most likely caused by the vane striking the ship's side during deployment, the vane flexing forcing the pump connector against the CTD frame's vertical member and breaking it. Subsequent dismantling of the pump showed it had flooded, the resultant short-circuiting of power and data lines producing the data spikes. The pump was replaced (by s/n: 054164) and the secondary instruments re-positioned inside the frame, conventionally fitted to the SBE 9+ fish.

E) Data spikes on the BBRTD channel had been getting progressively worse. Cleaning the connectors had some limited effect but did not eliminate the problem. The lead from the BBRTD to the BOB was replaced and cured the fault. Close inspection of the BOB connector of the cable indicated some water ingress causing the data loss.

F) The RDI WorkHorse Monitor ADCP's performed as expected for the duration of the cruise, with the exception of no Slave data in the following files:

D311_27s
D311_31s
D311_60s
D311_63s
D311_67s
D311_90s
D311_98s

Examination of the log file revealed no errors in the command file sent to the instrument, nor were there any errors or data problems with the corresponding Master data. Command files used throughout the cruise are attached. The exception was D311_063 where the communications lead was inadvertently disconnected before the command file was transmitted.
Note that LADCP data was only collected for CTD casts deeper than approximately 700m, the nominal range of the Ocean Surveyor 75kHz ship-fitted ADCP.

G) Copies of the Sea-Bird SeaSave configuration files are attached, one for the initial .CON file, one for the conductivity cell replacement .CON file, and one for the temperature sensor replacement. A separate .CON file is not included here (for the sake of brevity) when the altimeter was changed as it did not involve any change in coefficients.

Other instruments

1) Guildline Autosal 8400B salinometer, s/n: 60839. A total of 441 salinity samples were taken during the cruise for CTD analysis. The salinometer was sited in the Constant Temperature Lab, with the bath temperature set at 21C, 1 to 2 degrees above ambient temperature. Softsal was used as the data recording program for salinity values, and results were plotted via an Excel spreadsheet. Stn/cast 3/1, bottle 3 shows an anomalously low primary salinity value compared with the autosal and the secondary salinity channel. This was due to a data spike occurring at the exact moment of bottle firing as replaying the cast revealed. Stn/cast 67/1 shows a discrepancy between the Autosal salinity measurement and the values given by the CTD. This is probably due to contamination of the sample taken in marginal conditions.

6. Student projects - preliminary results

Sea surface temperature and salinities in Denmark-Strait

Between Iceland and Greenland, in Denmark-Strait two water masses meet; Polar Water from the Arctic Ocean and the Atlantic Water from the south.

To study the distribution of water masses and their mixing we sampled near surface salinity and temperature data with a thermosalinograph (TSG) every 30 seconds. The TSG was calibrated with CTD-Data and water samples drawn at the instrument's intake. The offset of the TSG is 0.144 for salinity and 0.04 for temperature. After some editing the data were averaged over 10 minute intervals.

In the TS-Diagram the two water masses can be clearly identified, the warm and saline Atlantic water and a nearly straight line of cold and fresh Polar water. Most of the data points are scattered around 3° C and 32.5 and indicate mixing between the Polar and Atlantic Waters.

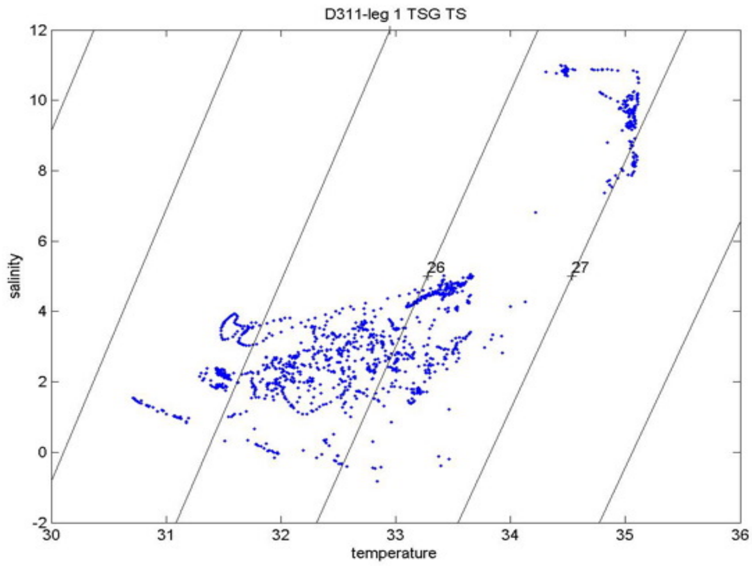

Figure 1: TS-Diagram from TSG-Data

The regional distribution of salinity and temperature shows the warm and saline Atlantic Water west and north of Iceland. It is carried by the Irminger-Current flowing from the south into the Nordic Seas. The cold and low salinity, down to 31 psu, water found at the continental slope of east Greenland, indicates the presence of Polar Water. It flows southward in the East-Greenland-Current.

Some low salinity water appears to turn eastward near 68°N and may be associated with the North Icelandic Current. In Denmark Strait the front between Polar and Atlantic Water is very sharp, while in the north the weaker gradients indicate mixing between the two water masses, possibly associated with meso-scale eddy activity.

West of the path of Polar Water, on the east Greenland shelf, surface salinities are again as high as 33.5, indicating a strong contribution of Atlantic Water. Recirculation of the Irminger-Current, a second separate current from the Atlantic or an eddy are possible scenarios. For an accurate identification we would need more measurements, such as CTD and current profiles.

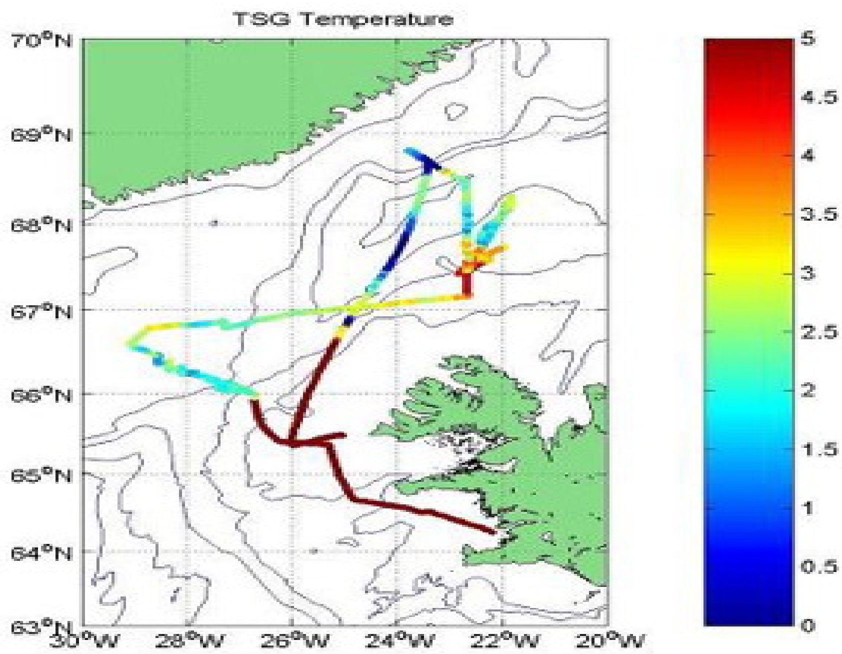

The mean (every 20 data) temperature after cleaning the output data.

Figure 2

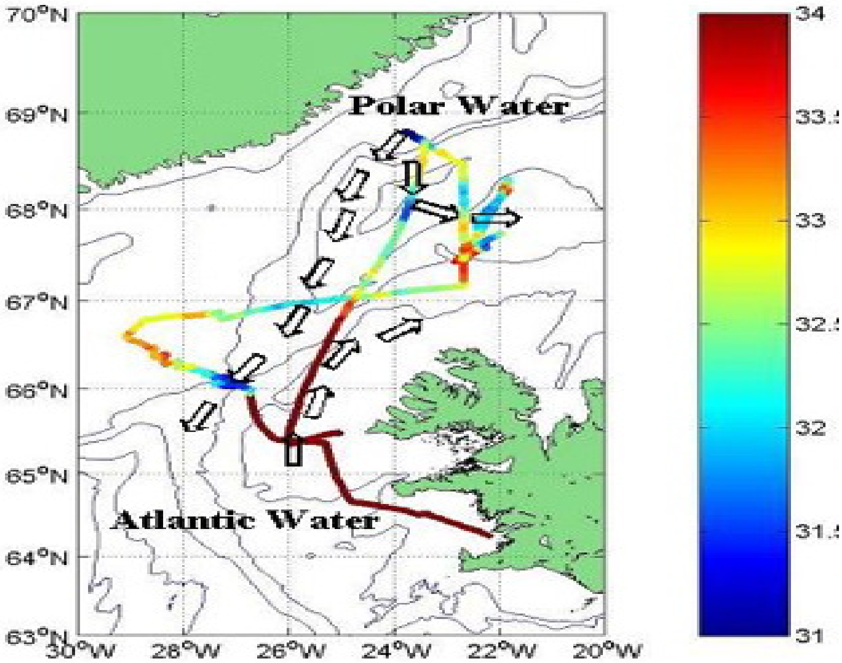

The mean (every 20 data) salinity after cleaning the output data

Figure 3

Sources of the Denmark Strait Overflow

An aim of the cruise D311 with the Research Vessel Discovery to the Denmark Strait was to determine the sources of the Denmark Strait Overflow Water. Here we present a preliminary attempt to determine theses sources using the data from two sections, one along the sill and one north of the Denmark Strait. Because of the adverse weather condition no stations were taken in the Iceland Sea and here we use data from profiling Argo floats deployed in October 2005.

The Overflow comprises dense waters from the Nordic Seas and the Arctic Ocean that cross the Greenland- Scotland- Ridge and sink into the deep North Atlantic, contributing to the NADW. To sink into the deep North Atlantic the water crossing the 600m sill in the Denmark Strait must be denser than 27.8. -S curves (Figure 4) and potential temperature and salinity sections taken at the sill (Figure 5, 6) show that the overflow temperature ranges from -0.3C to above 2 C and the salinity lies between 34.8-34.92.

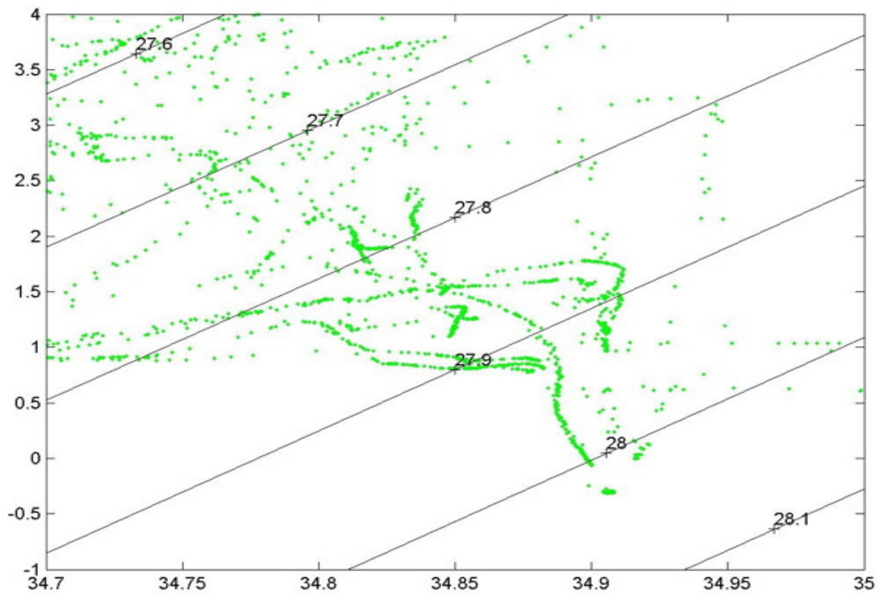

Figure 4: TS-diagram section 1 (sill of the Denmark Strait)

There are two principal hypotheses concerning its sources.

1) The origin of the Denmark Strait Overflow water (DSOW) is the East Greenland Current (EGC), which carries dense Arctic Atlantic Water and intermediate water from the Arctic Ocean. Recirculating warm but dense Atlantic Water from Fram Strait as well as colder dense Arctic Intermediate Water from Greenland Sea.
2) The main source is the intermediate water formed in the Iceland Sea, which then would provide the densest part of the overflow.

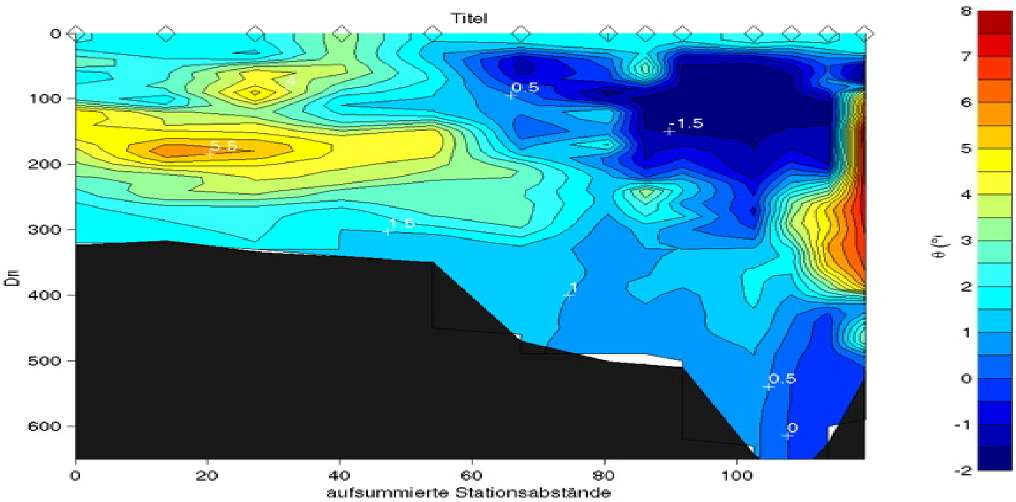

Figure 5: Distribution of Potential Temperature, section 1

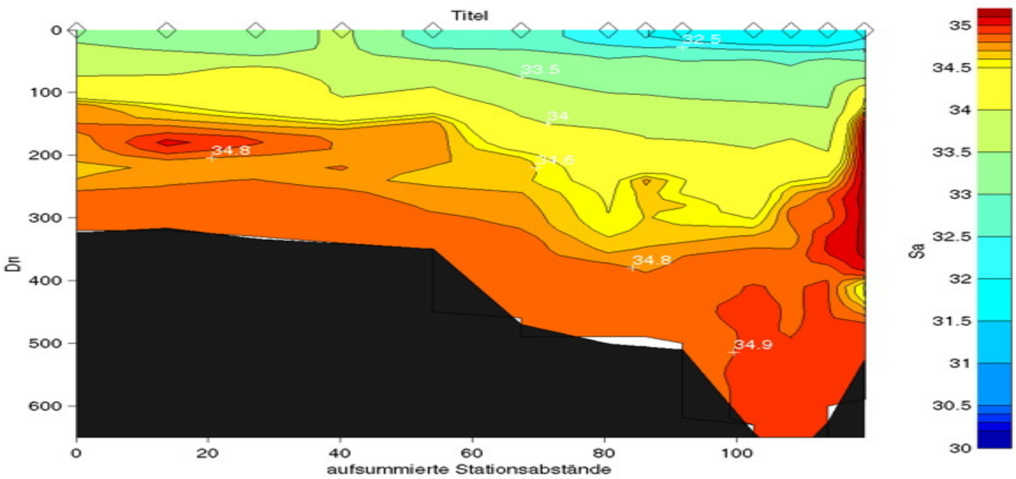

Figure 6: Distribution of Salinity, section 1

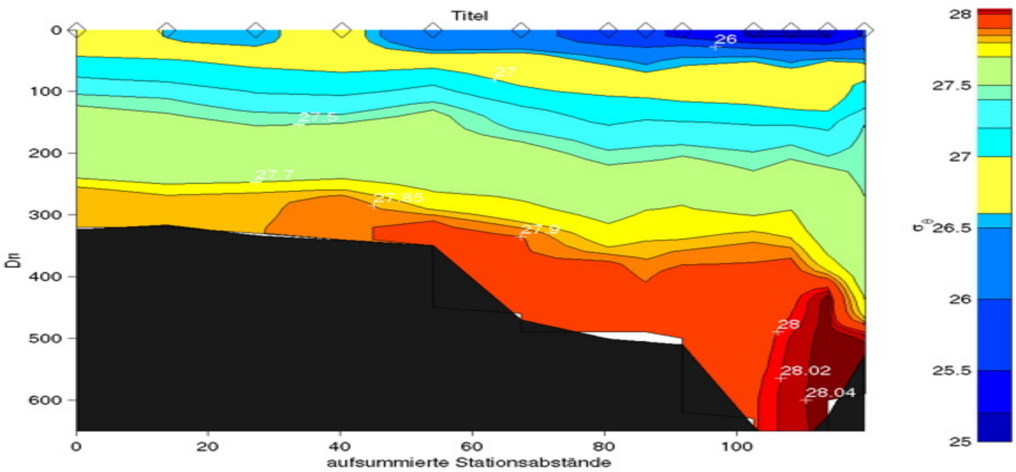

Figure 7: Distribution of Potential Density, section 1

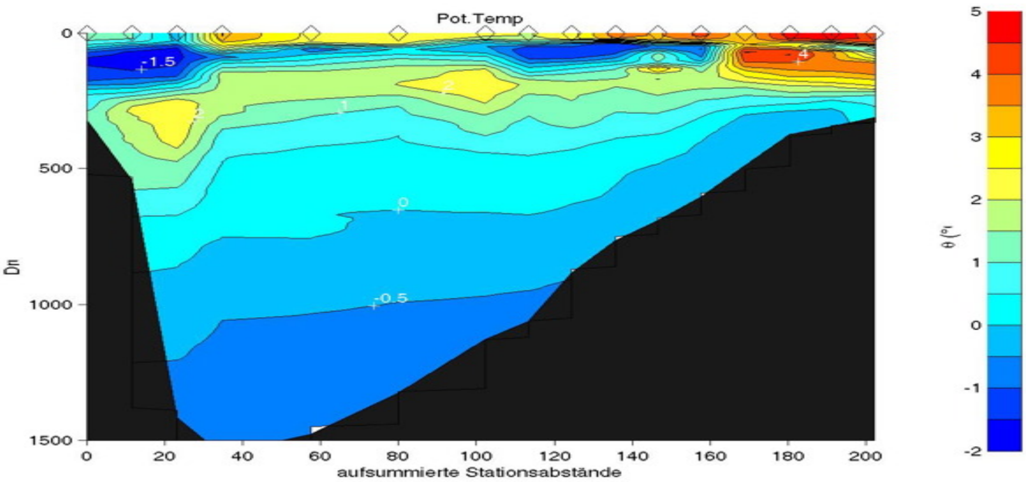

Figure 8: Distribution of Potential Temperature, section 2 (north of the Denmark Strait)

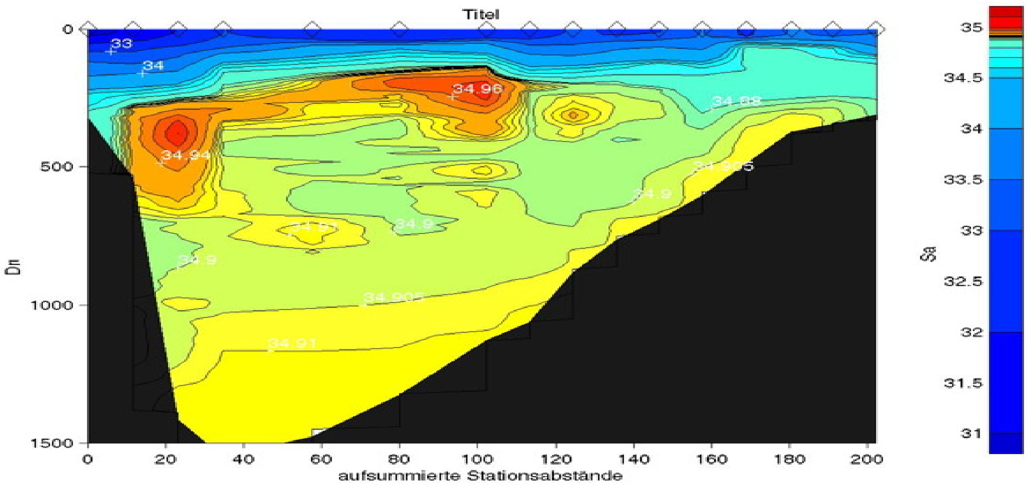

Figure 9: Distribution of Salinity, section 2 (north of the Denmark Strait)

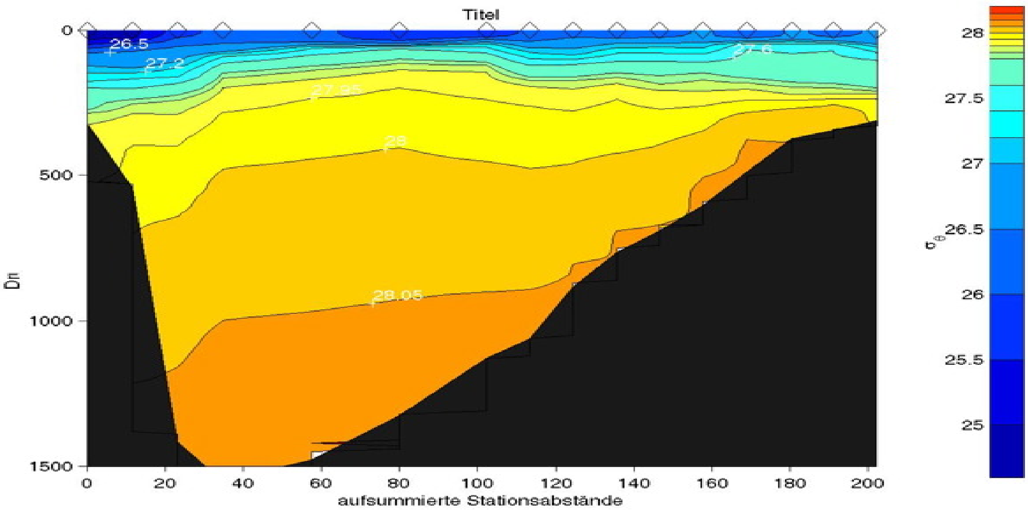

Figure 10: Distribution of Potential Density, section 2

The sections at the sill indicate that the densest water is found in the deep channel at the Iceland side of the strait (Figure 7) and section 2 (Figure 10) also indicates that dense water is found at higher levels above the Iceland slope. The overflow water also comprises warmer, more saline and less dense water (Figures 5, 6, 7) that could derive from the Atlantic Water recirculating in Fram Strait.

To distinguish between these two sources -S curves from the sill section (green), section 2 north of the sill (red), and from the floats in the Iceland Sea (blue) are plotted together. (Fig 11) These curves indicate that the Iceland Sea water column is too cold and has too low salinity to significantly contribute to the overflow. The East Greenland Current water masses, however, are similar to these found at the sill, both in the densest part as well as in the warm and less dense layers above.

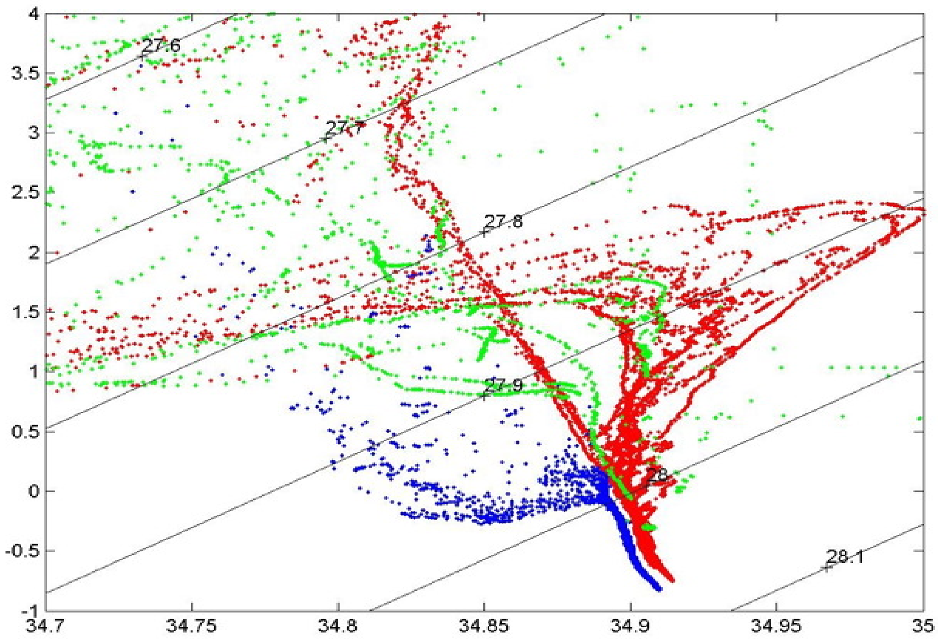

Figure 11: TS-diagram, blue: float data, green: section 1, red: section 2

This then suggests that the overflow, at least during the Discovery crossing mainly comes from the EGC. The densest part would then shift from the Greenland side to the Iceland side as the channel narrows and sill is approached. This is in agreement with the theory of channel flow crossing a ridge.

The water characteristics are determined from different data sets, the Discovery CTD data and the ARGO float, and there could be an error in sensor calibration, leading to the differences between the data. The area covered by the float tracks may not be representative for the part of the Iceland Sea that would contribute to the overflow. The float tracks suggest that the water recirculates in the Iceland Sea and, when leaving it rather moves towards the Norwegian Sea. The floats circulate at 1300m depth, which may not be representative for the water potentially contributing to the overflow. One way to remedy this would be to launch floats at the 300m level, which correspond to the density of the densest overflow water.

Seasonal Cycle of Water Mass Properties in the Islandic Sea -Observations and Mathematic Model

The Islandic Sea is the major source for Intermediate Waters in the Nordic Seas. These waters are formed through convection during winter and partly contribute to the overflow waters in Denmark Strait.

Since October 2005 continuous measurements of temperature and salinity profiles have been taken with ARGO profiling floats in the Islandic Sea. These autonomous floats drift at a depth of 1,000 m for a period of 10 days. They then sink to a depth of 1,300 m and ascent to the surface while measuring pressure, temperature and salinity at predetermined intervals (50 m steps from 1,300 m to 600 m, 25 m steps from 600 m to 500 m and 10 m steps from 500 m to the surface). At the surface the data and the GPS position of the float are transmitted via satellite to the ARGOS data centre. They then sink again to 1,000 m depth and the next drifting period starts. Figure 12 shows the surface positions of float No. 343.

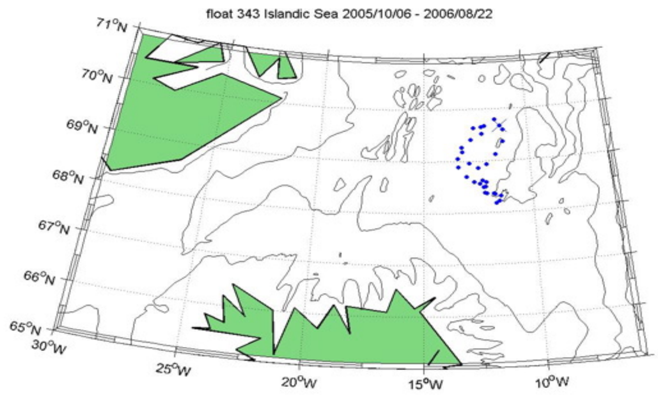

Figure 12: Positions of float 343 between 6th Oct. 2005 and 22th Aug. 2006

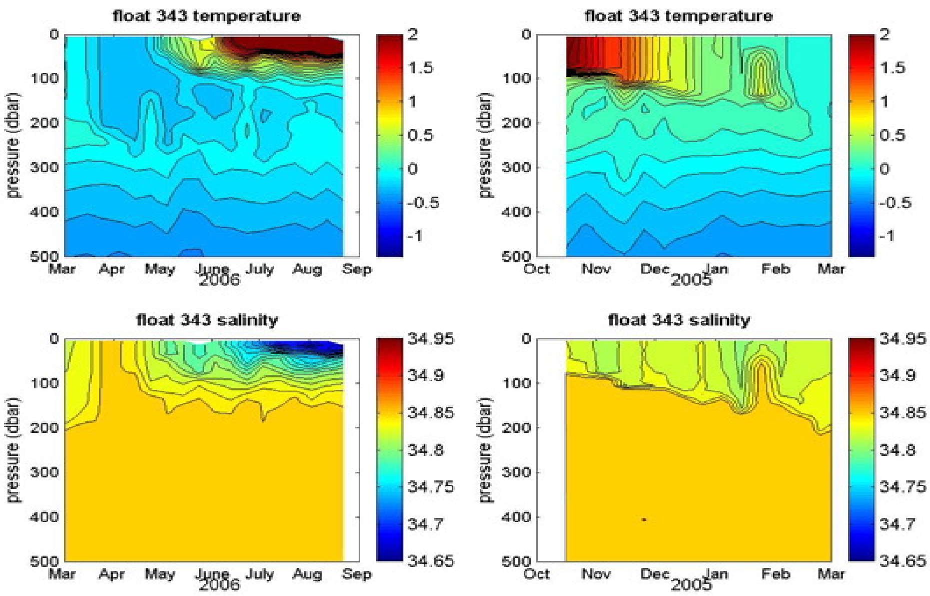

Figure 13: Seasonal Temperature and Salinity distributions from float data in 2005 and 2006

To illustrate the seasonal cycle of the stratification the development of temperature and salinity in the upper 500 m of the watercolumn are shown for the periods March to August and September to February (Figure 13). Solar radiation during the summer months heats the upper layer with temperatures increasing from about –0.5° C to more than 8° C. A strong seasonal thermocline is formed. During the winter month with little solar radiation and stronger winds the upper layer cools and deepens through convection. During late winter the mixed layer reaches down to approximately 250 m to 300 m.

The applied model of heat transport in a vertical water column is given by the equilibrium of the time change of temperature and vertical eddy diffusion (equation 1), and by the flux of heat at the sea surface (equation 2).

$$\frac{\partial T}{\partial t} = \frac{\partial}{\partial z}\left(A(z) \cdot \frac{\partial T}{\partial z} \right) \qquad (1)$$

$$W = -A(z) \cdot \frac{\partial T}{\partial z}, z = 0 \qquad (2)$$

T = T (t, z) and A = A(z) denote time and depth dependent temperature and the coefficient of eddy heat diffusion, respectively. W (t) denotes the flux of temperature at the sea surface. This quantity is proportional to the heat flux. Having main features in view, this model is used for reproducing seasonal variations of temperature profiles as having been observed by floats in the Icelandic Sea.

It is assumed that the heat flux is sinusoidal with a period of one year, taking the value zero in March. The value of the coefficient of eddy heat diffusion is prescribed as constant from the sea surface down to a depth of 200m, decaying from there exponentially to the exp(-2)th part of the upper mixed layer value at the sea bottom (500m). The differential equation (1) with boundary condition (2), representing time dependent forcing, is treated numerically. For this purpose the first order time derivative is replaced by a forward difference and the second order space derivative by a second order central difference. In (2) for the first order derivative a one sided difference is applied. The resulting time stepping procedure is performed using a time step Δt = 50 s and spatial grid point distance Δz = 10 m. Therefore, there are 50 depth levels at which the temperature is computed, and 630,720 time steps are needed to complete the cycle of a year. As cooling will lead to instabilities, convection must be considered in the model, too. This process is included into the model by a mixing mechanism having to be performed at the end of every time step.

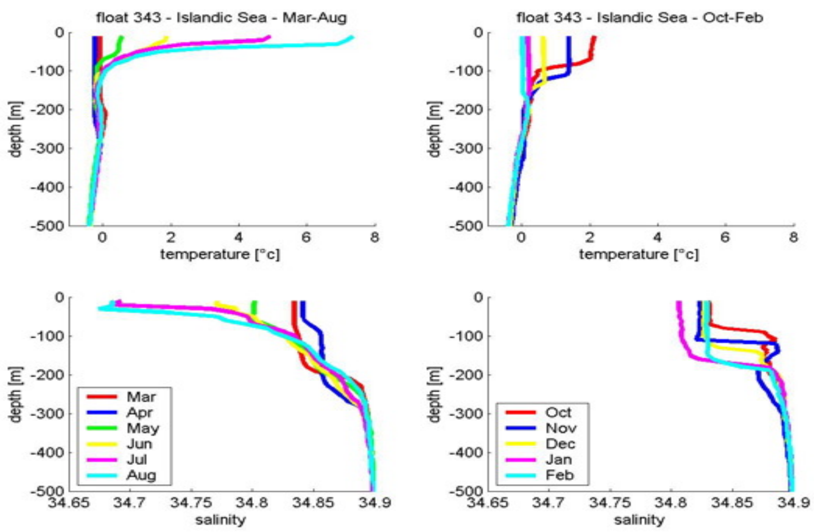

Figure 14: Temperature and Salinity profiles from float data

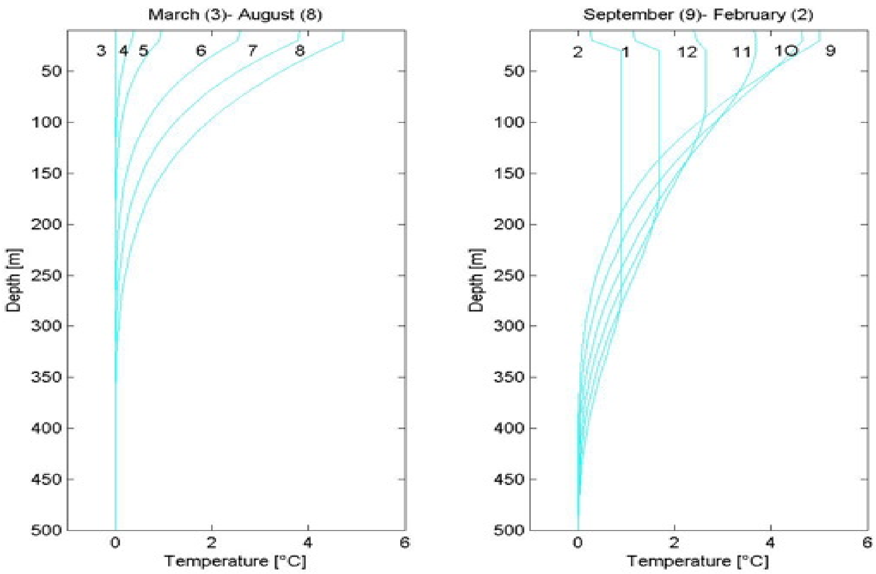

Figure 15: Seasonal Temperature profiles computed by the model

Figures 14 and 15 show the observed (14) and the computed (15) temperature profiles for the months March to August and for September to February, respectively. Although important processes having been neglected necessarily in this spatially one-dimensional model, e.g. advection and explicitly represented convection, the profiles reflect some characteristic features of observed profiles.

To these belong the typically seasonally development of the temperature profile close to the surface. In summer a distinct warm water mixed layer appears with a strong vertical gradient at 100m depth, which, however, is weaker than in the observations (see Fig. 14). This might be due to the coefficient of heat diffusion having been chosen too large in depths down to 200m. The surface temperature decay begins in September and properly reflects the observed one. The degradation of the stratification in winter and the typical deepening of the upper homogeneous layer is well reproduced by the model. This realistic deepening is brought about by the proper parameterisation of convection in the model.

It is straightforward to extend the model by also considering the change in time of salinity at the different depth levels. The numerical model for salinity only differs from that one for temperature by changing the dependent variable and by including salinity flux instead of W(t). Moreover, values for the coefficient eddy salt diffusion might be chosen which differ from those used for eddy heat diffusion. Applying the convection mechanism in the combined temperature-salinity model requires computing the density by applying the equation of state at the end of every time step.

Freshwater Transport in the East Greenland Current

Global warming can cause dramatic climatic changes on earth. One change might be increasing freshwater entries in polar regions. A freshwater top layer would isolate the underlying warm water masses coming from the south. Due to this the North Atlantic Current (the northern offshoot of the Gulf Stream) would not cool down (become dense) and sink to the deep. This would weaken, and perhaps stop, the Atlantic Meridional Overturning Circulation (AMOC). Such changes may be detected by an increase in the freshwater transport in the East Greenland Current, which carries the freshwater from the Arctic Ocean and from Greenland ice melt to the North Atlantic. So it is always expedient to monitor the current freshwater transport in the Nordic seas. We calculated the freshwater transport in the East Greenland Current, using data obtained on leg_2 of the RRS Discovery cruise D311.

Section 1, stations 43-48, 23.09.06-24.09.06

Station 43: 63°10,50' north
41°01,08' west

Station 48: 62°54,93' north
40°16,18' west

The measurements of temperature, salinity and depth recorded at the stations give us the thermo-haline structure of the East-Greenland Current on the shelf. We only considered the upper 200 m .To find geostrophic velocities we use the dynamical method the specific volume anomalies and the geopotential anomalies. Before that however, we present the temperature, salinity and TS structure of the section (see Fig.16, 17, 18). Figure 16 shows that from the surface down to 160 m depth we have cold water up to station no. 46.

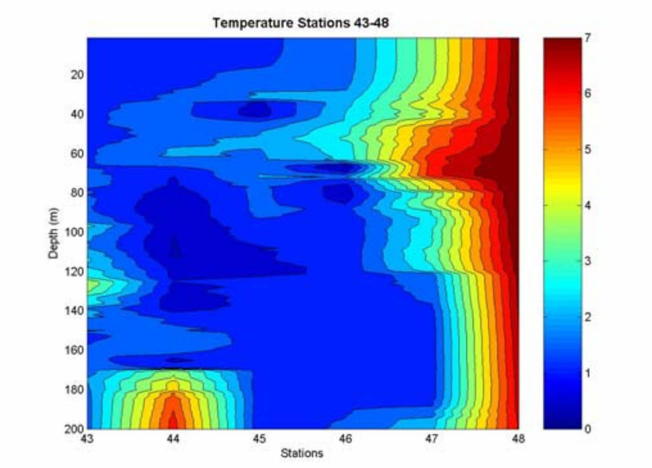

Figure 16: Temperature distribution along the section

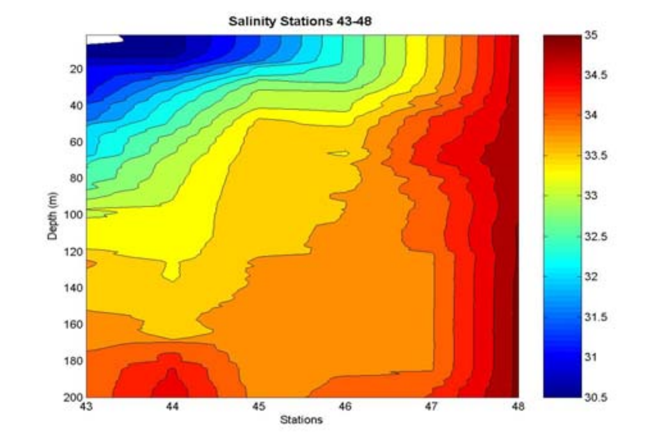

Figure 17: Salinity distribution along the section

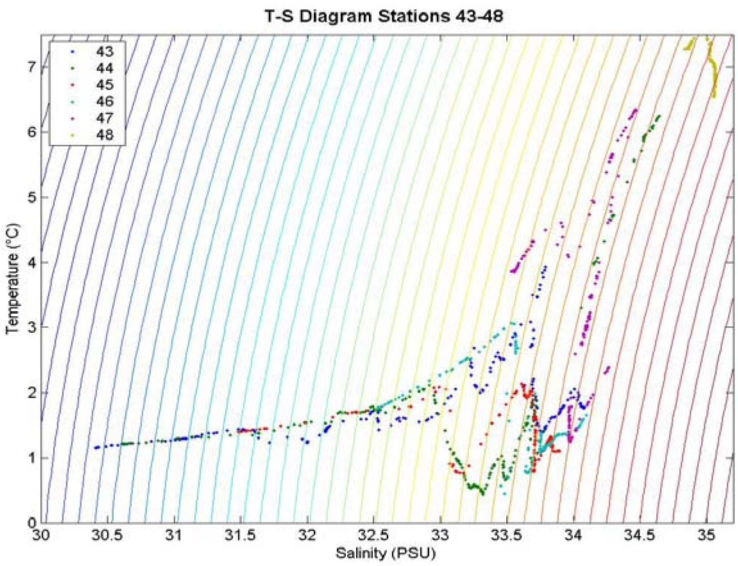

Figure 18: TS-diagram along the section

Looking at Figure 17 at this section we have low salinity between station 43-44. The interesting part can be localised in the upper region down to 90m from surface on. So we can concentrate on this zone of the East Greenland Current. In all three figures Atlantic Water and Polar Water can be clearly identified by their typical temperature, salinity and density values (Figure 19). To estimate the freshwater transport we have to determine the velocity of the current. Here we assume that the current is in geostrophic balance and that the velocity is zero at 200 meters. The barotropic part of the current is neglected.

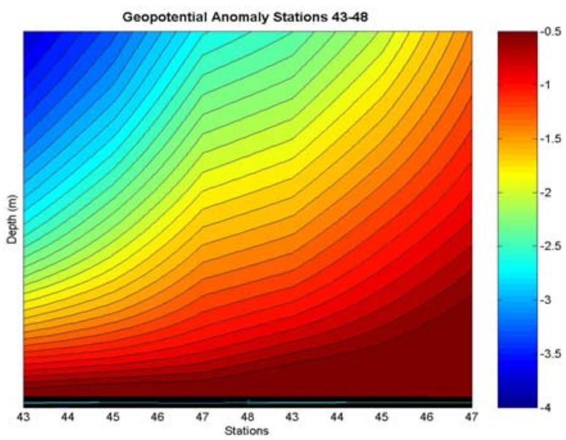

Figure 19: Geopotential Anomaly along the section

To discuss the geostrophic method we first introduce the concept of geopotential.
It is defined as the amount of work required to lift a mass M over a vertical distance dz against the force of gravity disregarding on friction.

$$dw = M \cdot g \cdot dz$$

(g = 9,81 m/s^2, M: Mass, w : quantity, dz: vertical distance). So the geopotential (Φ) is defined by:

$$Md(\Phi) = dw = M \cdot g \cdot dz$$

It is given in joules/ kg or m^2/s^2. That means it represents potential energy changes per unit mass over a vertical section.

$$d(\Phi) = g \cdot dz = -(\alpha) \cdot dp$$

$((\alpha) = 1/(\rho))$. Integrating from ρ_1 to ρ_2 and writing $\alpha = \alpha_{35,\,0,\,p} + \delta\alpha$.We get:

$$- \Delta\,(\Phi)_{std} - \Delta\,(\Phi).$$

The first part is the standard geopotential equal on all stations. The second part gives us the geopotential anomaly (Figure 19) and is a function of S,T and p, given in dyn m; 1 dyn m = 10.0 J/kg. Use D for geopotential and using dynamical m, $(D_2 - D_1)$ is close to $(z_2 - z_1)$. The geopotential anomaly is first computed relative to the sea surface. To conform with our assumption of no velocity at 200 m, the zero level has to be moved to this depth. This leads to a sea surface slope from Greenland towards the shelf break of about 20 cm over the section.

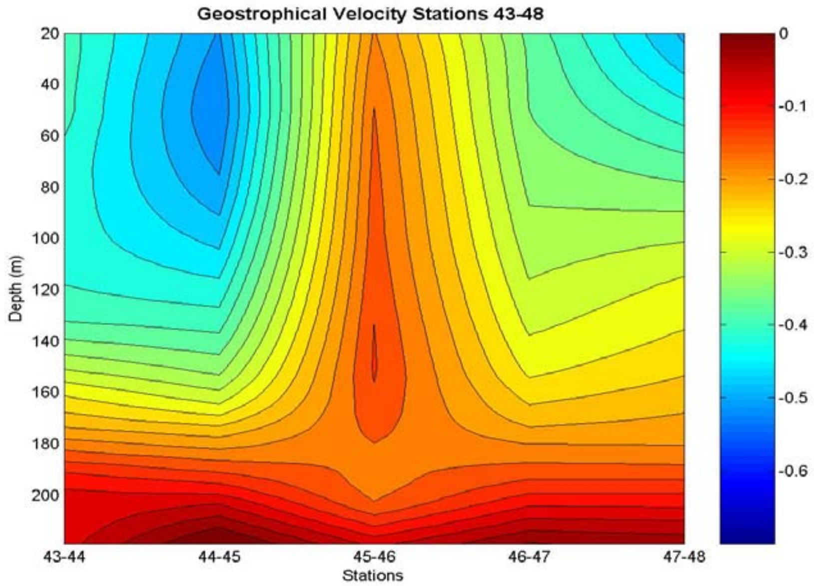

Figure 20: Geostrophical Velocity along the section

Figure 20 plots geostrophical velocity. It shows, in combination with Figure 19, that we have a strong gradient between 120m and 140m depth, so we concentrate on this wedge. At the end by 200m we have no geopotential anomaly, because in this depth the gradient of geopotential anomaly is set to zero.

In this phase we calculate the geostrophic velocity sheer (V_1–V_2) between two levels 1 and 2 and the stations B and A.

$$(V_1 - V_2) = \frac{10}{L \cdot 2 \cdot \Omega \cdot \sin(\Phi)} \cdot (\Delta D_B - \Delta D_A)$$

We calculate the geostrophic velocity from the horizontal gradients in geopotential anomaly, recognising that it is relative to the surface.
Figure 20 shows the geostrophic velocity between stations 43 and 48. At the surface between stations 43 and 45 we can see, that the geostrophic velocity is higher than in the part of station 45 to 48. The geostrophic velocities show two high speed cores associated with low salinity there. One over the shelf break indicating another part of the East Greenland Current. We know that the water masses moves southwards but with different velocities. In this case we have to recognise that in geostrophic approximations

the velocity at bottom has been set to zero (here at 200m depth). In reality we find a velocity at the bottom, so also friction.

$$\sum_{j=1}^{m}(\sum_{j=1}^{n} 1 \cdot \frac{\Delta D_{(j+1)i} - \Delta D_{ji}}{f} \cdot \frac{35{,}2 - S_m}{35{,}2}))$$

(for S_m = mean salinity between j+1 and j). This formula includes all parts we calculated.

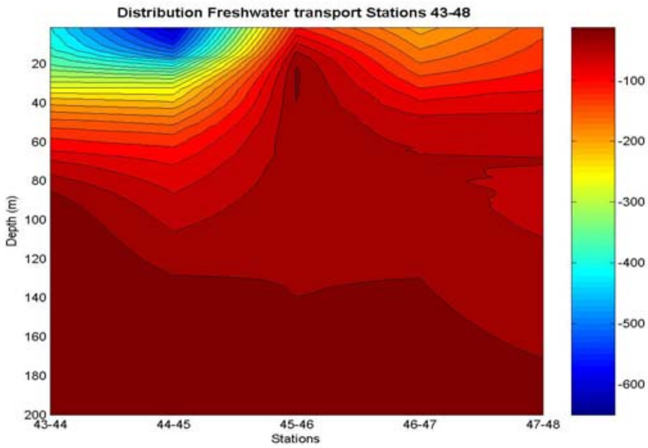

Figure 21: Freshwater distribution along the section

We also used the Coriolis parameter f (= 2 Ω sinϕ) which is f = 0,00013 1/s, for this latitude.The freshwater transport is given per 1 m layer in Sv (Sverdrup; = 10^6m³/s), it is shown in Figure 21.The total transport of freshwater through the section is 0,06 Sv.We notice, that freshwater transport is much more concentrated to the surface than at the bottom with a difference from 0 to 600 m³/s. We can conclude that Polar freshwater ,which is flowing southwards, mostly can be found in a wedge close to Greenland from surface down to 90 m depth on this section of the East Greenland Current, from here on the content of freshwater is decreasing rapidly.

Our result absolutely lies within the expected bounds, bearing in mind we only calculated the geostrophic part of the transport. Additionally we may hypothesise a contingent future evolution: In case of decreasing freshwater input, the stability of the stratification would decrease. From here on it would be easier that deep water masses mix with the surface layer and the thermohaline circulation would be unhinged. This would facilitate convection at high latitute and thus increase the strength of the thermohaline circulation. The salinity at the surface would get higher rates and we could recognise a faster convection. In case of increasing freshwater input we hypothesise that the convection may be reduced. The thermohaline circulation would then weaken, leading to a smaller transport of warm surface water towards the Nordic Seas and the Arctic Ocean. But this is only in the upper northern seas. To get more information about the freshwater transport in the East Greenland Current and its behaviour, different measurements are used. A good method of measuring the freshwater signal is using a combination of seacats and current meters.

Air Sea Heat Fluxes

During our cruise we measured the sea surface temperature every 30 second. The temperature ranged between 14.275°C and -0.99°C with a high variability on small scales. Generally there are three main reasons why the water temperature changes:

a) Advection
Currents move different water masses with different temperatures and heat is transported horizontally.

b) Vertical mixing
Vertical mixing between water layers can result in vertical heat transport.

c) Heat exchange with the atmosphere
Latent and sensible heat fluxes between the water and the atmosphere and radiative fluxes change the upper ocean temperature.

The question we asked ourselves was to which degree the heat fluxes between the ocean and the atmosphere are responsible for changing the sea surface temperature.

The heat fluxes between ocean and atmosphere can be computed with bulk formulas, including the total irradiance (Q_{tir}), the latent and sensible heat flux (summed up as Q_{turb}), the longwave incoming radiation (Q_{lin}) and the longwave outgoing radiation (Q_{lout}).

$$Q_{heatflux} = Q_{tir} + Q_{turb} + Q_{lin} - Q_{lout}$$

The ship's instruments measured the position (latitude, longitude), the wind speed, the sea surface and the air temperature, the air pressure, the humidity and the total irradiance.
The latent and sensible heat flux was computed following *Winsor and Björk (2000)*:

$$Q_{turb} = \rho_a * c_h * c_p * u_a * (T_a - T_s)$$

ρ_a = density of air, c_h = heat transfer coefficient, c_p = specific heat of air, u_a = Wind speed, T_a= Air temperature, T_w = water temperature

The longwave incoming radiation has been computed as

$$Q_{lin} = \varepsilon_a * \sigma * T_a^{\ 4} \quad , \quad \varepsilon_a = 0.7829 * (1 + 0.2232 * Cl^{2,75})$$
$$= 0.7829 * (1 + 0.2232 * Cl^{2,75}) * \sigma * T_a^4$$

*T_a = air temperature, σ = 0.826 * 10^{-10}, Cl = cloud coverage, ε_a= emissivity of the air*

The cloud coverage was estimated by scientists and members of the ship crew; we compared two values here (60% and 75%, see *Discussion*).

The longwave outgoing radiation was computed using

$$Q_{lout} = \sigma * T_s^4$$

*σ =0,826 * 10^{-10}, T_s = water temperature*

Finally the heat needed for the fluctuations of the sea temperature (Q_{sea}) was computed using

$Q_{sea} = \rho_w * c_w * (\Delta T / \Delta t) * d$

ρ_w = water density, c_w = specific heat of water, ΔT = temperature change, Δt = time period, d = upper water layer depth

The upper water layer depth was estimated to a value of 50 m. Furthermore we calculated a 1 hour mean for Q_{sea}. Figure 22 shows the total heat flux ($Q_{heatflux}$) with its single components.

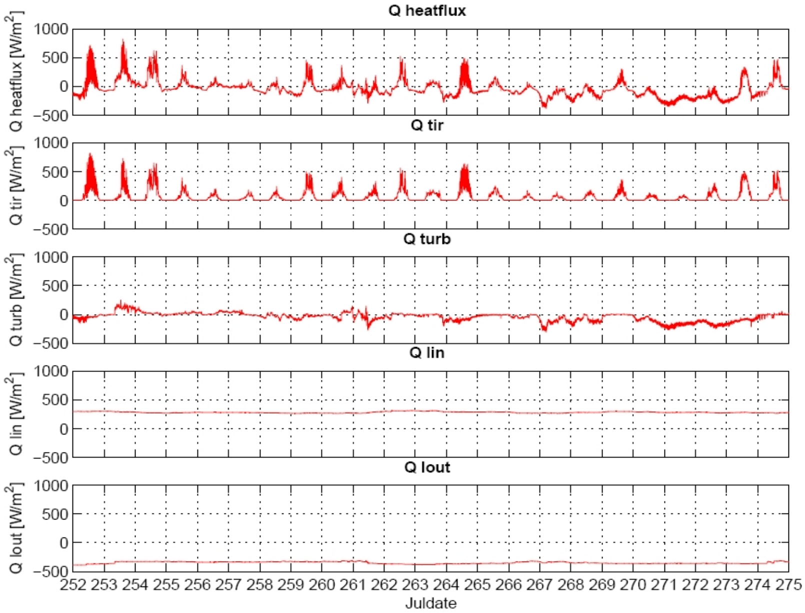

Figure 22: Heat Flux Q and its components

The heat flux has daily cycles, reaching from 820 W/m^2 to –387 W/m^2. This is mainly caused by the strong total irradiance during daytime and the lonwave outgoing radiation during the night.

The daily mean heat flux, which we plotted in an additional graphic, shifts from INTO the ocean to INTO the atmosphere during the cruise. This agrees with a general shift from the water-heating summer times to the water-cooling winter times. We were able to detect the change of these two periods, compare with Figure 23.

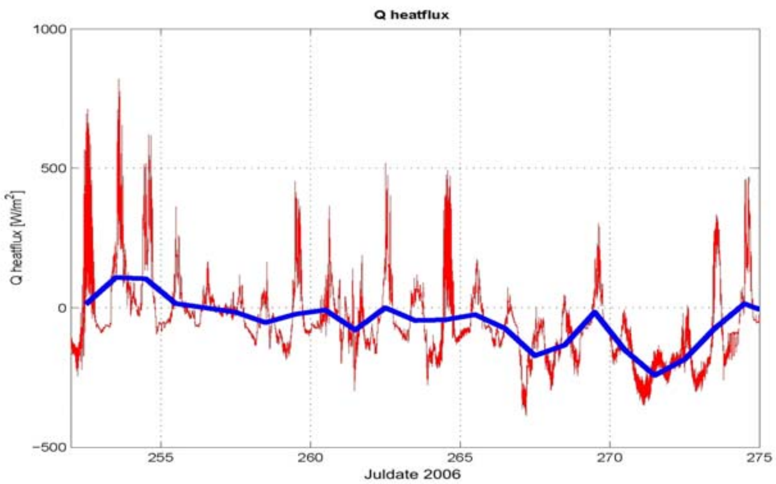

Figure 23: Heat Flux and its daily mean

We calculated the overall mean heat flux. It has a value of –46 W/m^2, which means a heat transfer from ocean to atmosphere. Figure 24 shows among other things the total air sea heat flux and the 1 hour mean for Q_{sea} during the whole cruise. On short time scales the air sea heat fluxes are not correlated with the heat fluxes needed to explain the ocean temperature change. The air sea heat fluxes fluctuate between –400 and 800 W/m^2, whereas the Q_{sea} values range between +/- 100 000 W/m^2. Therefore the air sea heat flux cannot be the main reason for the detected water temperature changes during our cruise.

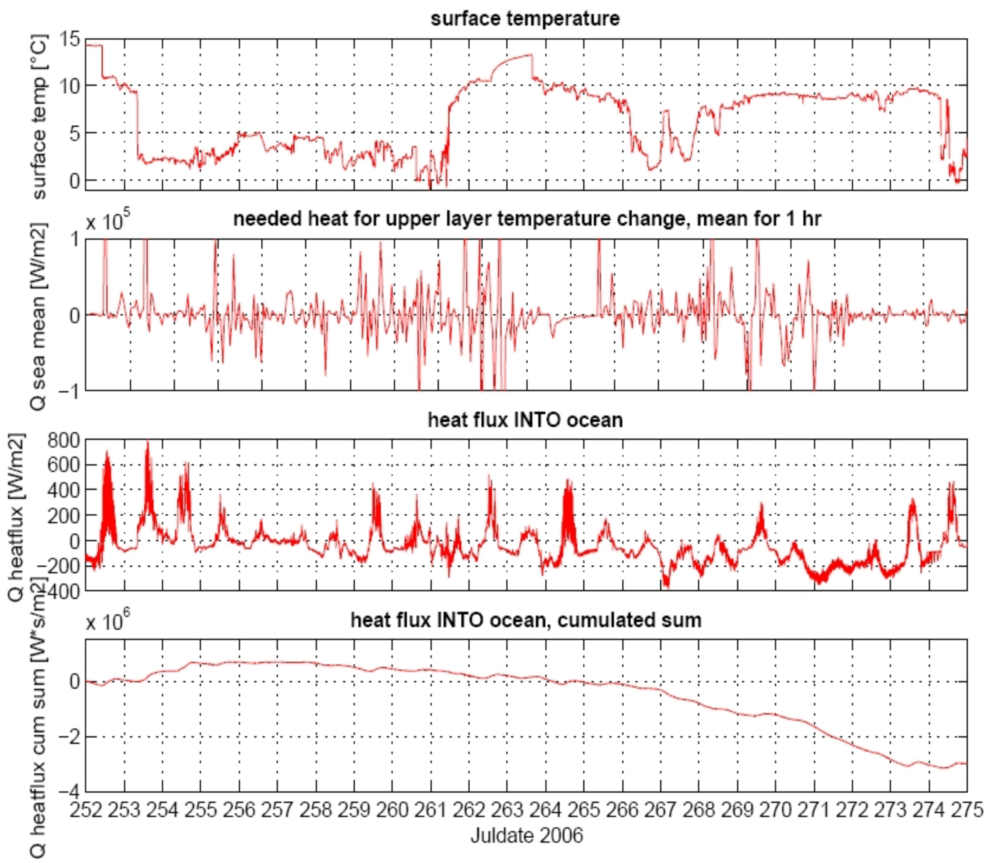

Figure 24: Surface Temperature, Q sea mean (1hr), Q heatflux, Q heatflux/cumulated sum

After Q_{sea} was compared with $Q_{heatflux}$ for the whole cruise, we concentrated on two other illustrative comparisons:

a. We checked the temperature delta (ΔT = 0.376°C) from a geographic position(67.0339 N, -24.7533 W) we crossed and measured two times with a gap of 5,67 days (255 16:44:00, 261 08:48:00). The motivation behind this was to be more secure that we measured the same water mass. The temperature increases by 0.376°C within this period, resulting in mean Q_{sea} of 158 W/m^2. This is supposed to be caused by strong incoming radiation, however the heat flux was in the opposite direction and cannot explain the heating of the water, see Figure 25. We assumed the heat fluxes kept the same, even though we did not hold our position.

b. Furthermore, we compared the $Q_{heatflux}$ and Q_{sea} of a short time period of 6 hours. Figure 26). During the chosen time slot, from day 263 00:00:00 to 06:00:00, the sea surface temperature slowly increased from 12.643°C to 12.931°C, which results in a Q_{sea} of 1000 to 4000 W/m^2. But within the same period a negative heat flux, in line with a heat transfer into the atmosphere, was computed. The values are about 75 to 120 W/m^2. That shows that neither the amount of heat flux nor its direction can explain the temperature decrease.

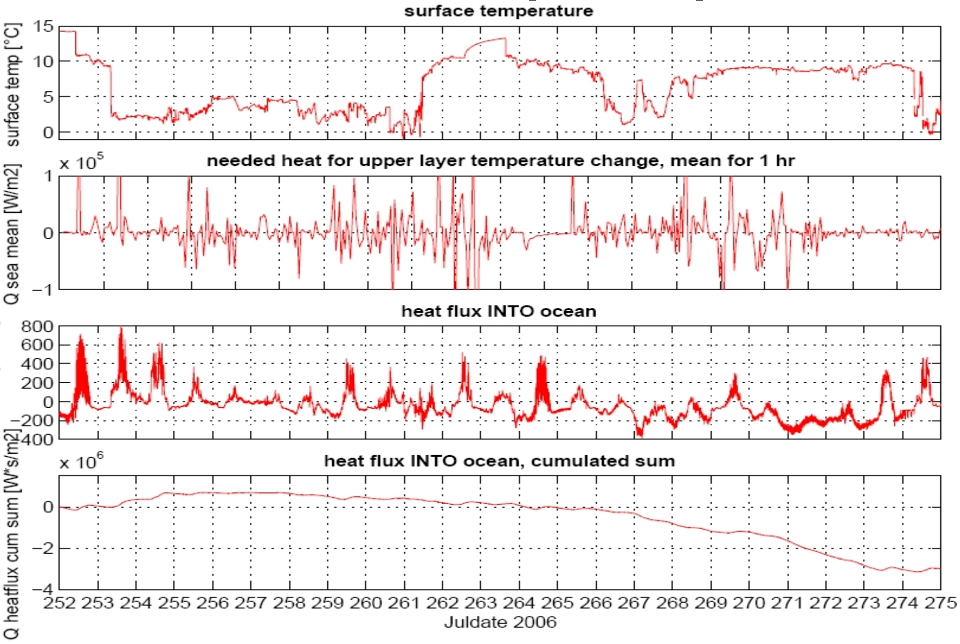

Figure 25: Q heatflux, Q heatflux/cumulative sum for a choosen geographic position (67.0339 N, -24.7533W) we crossed twice

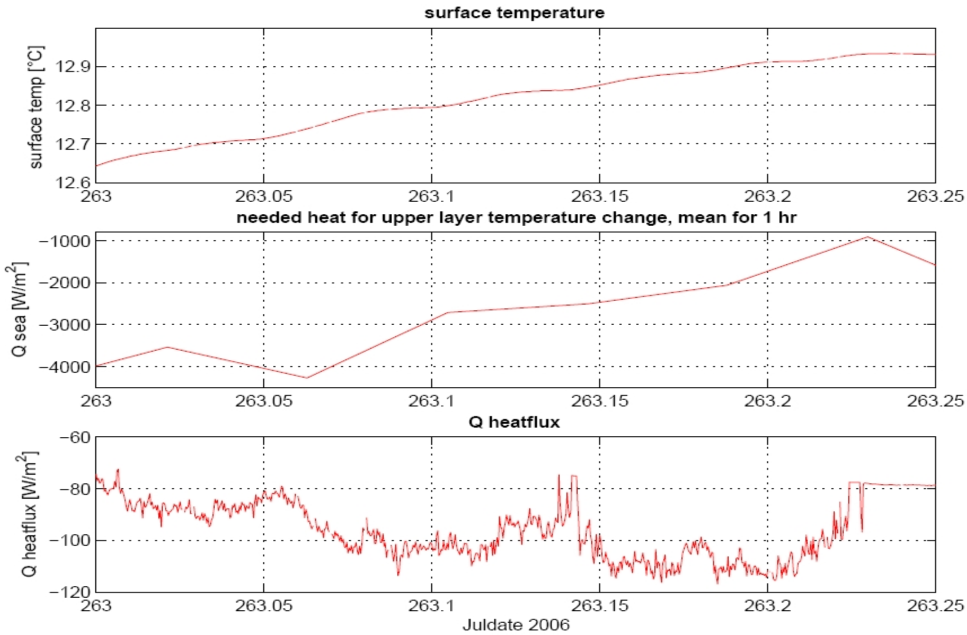

Figure 26: Surface temperature, Q sea mean (1hr), Q heatflux during the chosen time period from day 263 00:00:00 to 06:00:00

Our work on the total heat fluxes certainly shows the transition from summer to winter. The curve of the daily mean falls from the positive into the negative domain. Also, the overall mean heat flux with a value of –46 W/m^2 shows the negative heat balance, characteristically for this season and latitudes.

Nevertheless, we have a few uncertainties in our estimations, that are in particular the cloud coverage and the upper water layer depth that we needed for computing Q_{sea}.
There was no measurement of the cloud covering, that's why two calculations with 60% and 75% mean covering where done as a comparison. The resulting mean heat fluxes are –33 and –46 W/m^2, a difference of more than 40%.

Another estimation was done with the depth of the upper water layer. The needed heat for the measured temperature change strongly depends on the estimated water layer depth. We took a depth of 50 m for our computing, which seems to be reasonable. Further work on CTD data could probably improve this estimation.

During our cruise the vessel was located in different water regimes with different sea surface temperatures caused by ocean currents. It is sure that advection of other water masses plays a huge part in heat transport in this area. That is also one reason why we could not find a correspondence between the heat fluxes and the sea surface temperature. Finally there could be heat transport by vertical mixing between water layers, which we also left out of consideration.

Interpolation methods for hydrographic sections across a sloping bottom

The aim of cruise D311 in the Irminger Sea was to measure transports and mixing in the overflow through Denmark Strait. One method to estimate volume, heat and freshwater transports of the overflow is to use hydrographic sections across the dense plume south of Denmark Strait. CTD measurements provide a good vertical resolution. However, since they are time-consuming, the sections usually consist of only few vertical profiles leading to low horizontal resolution. When transports are calculated, the stations need to be interpolated across the section. The overflow plume runs along the Greenland shelf slope, thus profiles at different depths are taken. The common horizontal interpolation of these profiles is problematic at the bottom where the overflow water is situated.

The aim of this project is to apply two alternative interpolation methods for hydrographic sections across a sloping bottom. This may improve the calculation of heat and freshwater transports. An improved interpolation could then be used to find the minimum number of profiles in a section needed to estimate transports within a given error range.

The following interpolation methods are applied to the standard hydrographic section ASOF 3 recorded in 2005. This section is situated 500 km downstream of the Denmark Strait sill and consists of 15 stations spaced over 175 km. As an example interpolations are carried out for the temperature field.

The common horizontal method interpolates the temperature field along isobars (Figure 27). The results are reasonable for surface and intermediate layers. In the bottom layer, parts of the temperature field are missing that cannot be interpolated due to different profile depths. These are the triangles that are formed by the intersection of real bottom (red line) and the bars corresponding to each station. The step-like structure of the bottom is also found in the interpolated temperature field close to the bottom where the isotherms are strongly inclined. The overflow plume is not described realistically with the interpolation along isobars.

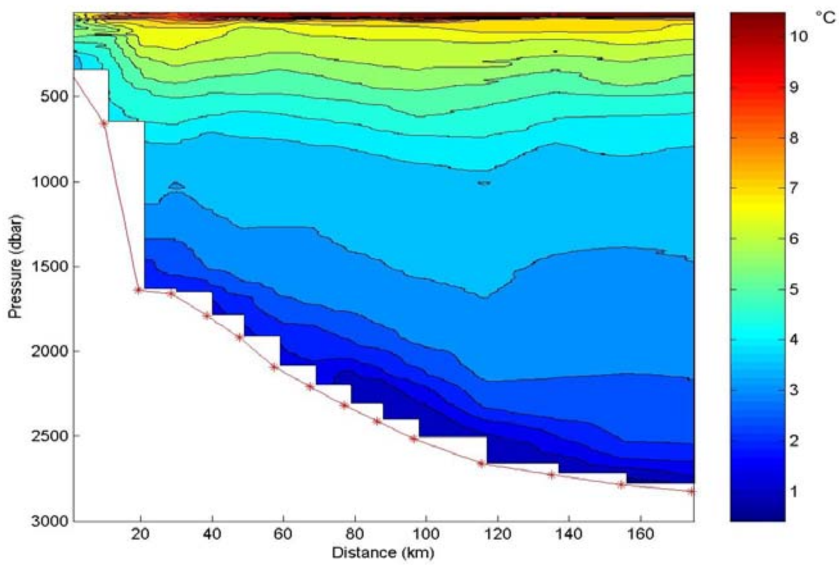

Figure 27: Temperature field from interpolation along isobars (red line indicates the bottom)

The interpolation of the bottom layer can be improved by taking the bottom pressure of each station as reference level (Figure 28). With this transformation, the isotherms close to the bottom are nearly horizontal. A horizontal interpolation now produces appropriate results for the temperature distribution in the overflow plume. Finally, the temperature field is transformed back to the isobaric levels (Figure 29). However, the step-like structure appearing in the bottom layer using the common interpolation is now shifted to the surface. The lower part of the resulting temperature distribution can be used to calculate the heat transport of the overflow plume.

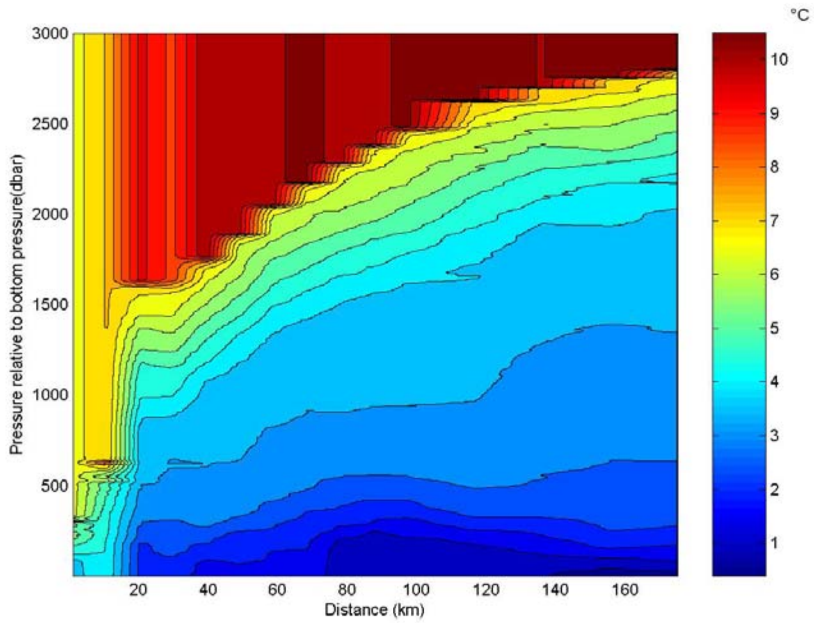

Figure 28: Bottom pressure as reference level

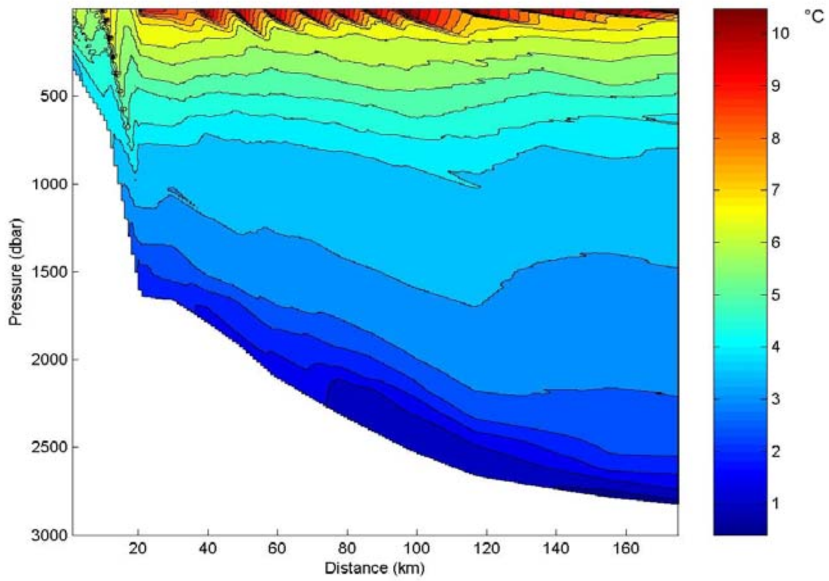

Figure 29: Interpolation with the bottom pressure as reference level

When the heat transport of the whole section is to be computed, an appropriate temperature field can be obtained combining the resulting upper layer of the first and the lower layer of the second method. However, this mixture of methods may cause problems at the interface.

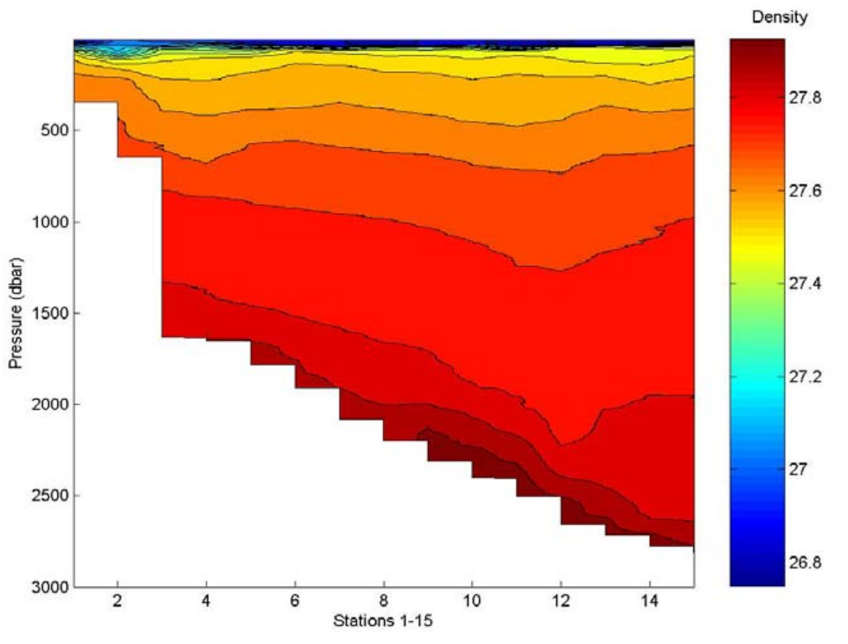

Figure 30: Density distribution

The density distribution of the section (Figure 30) suggests another approach would be to interpolate along lines of constant density. This can be accomplished by a transformation of the temperature profiles from pressure into density space. This transformation, the interpolation in density space and the back transformation are described below.
The dependence of density on pressure determines the transformation. As the density values in the profiles are not monotonically increasing, they are sorted to increase with

increasing pressure. This makes sense physically as we do not expect instabilities. The temperature values are sorted simultaneously with the same index. To establish a unique transformation between density and pressure coordinates, density values are rounded to 10^{-4} kg/m^3 and the temperatures corresponding to constant density values are averaged. The temperature profile for each station is interpolated to a density grid with a spacing of 10^{-4} kg/m^3. The temperature field is interpolated horizontally, i.e. along the isopycnals (Figure 31). The interpolated temperature field in density space is transformed back to pressure space by averaging over 1dbar bins (Figure 32).

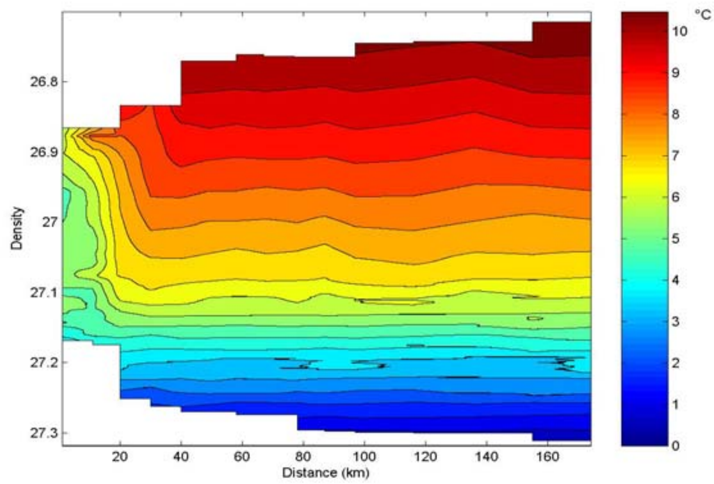

Figure 31: Interpolation along isopycnals

In the areas where density changes only little within a large pressure range, the back transformation to a 1dbar grid causes a loss of temperature values. These can be seen as empty values in the temperature distribution shown in Figure 32. However, as this happens in regions of small gradients, the missing values can be linearly interpolated. Figure 33 shows the final result.
The interpolation along isopycnals does not produce a step-like structure in the overflow plume. It fails where isopycnals intersect the bottom or the surface. In density space (Fig. 31), this corresponds to the step problem for different bottom depths in pressure space.

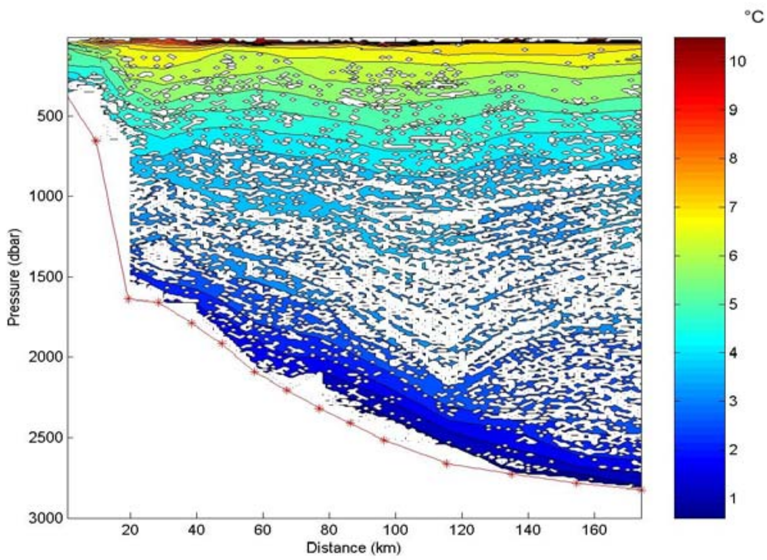

Figure 32: Interpolation along isopycnals

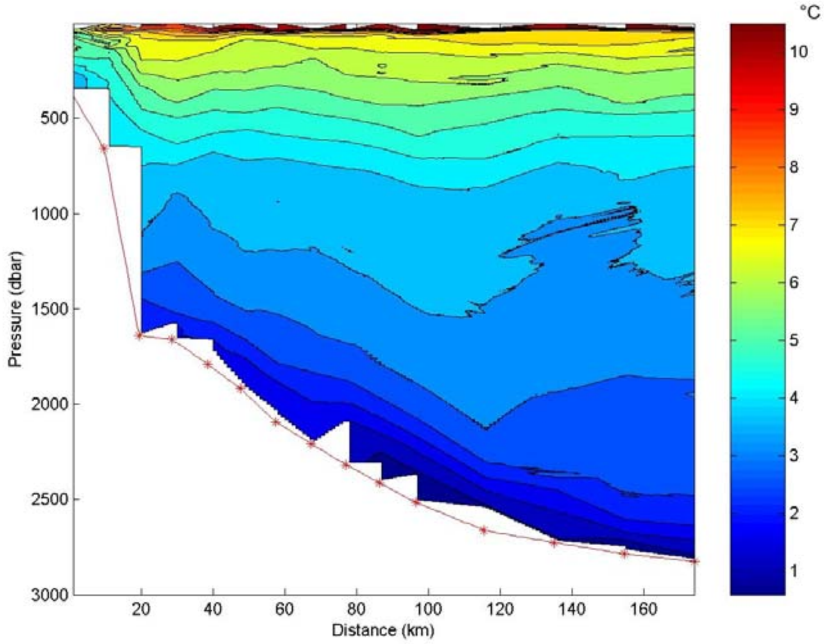

Figure 33: Vertically interpolated temperature field from interpolation along isopycnals

The interpolation relative to the bottom pressure and along isopycnals are both an improvement compared to the interpolation along isobars where the bottom layer is concerned. The two methods adapt the structure of the sloping isopycnals in the bottom layer. However, we do not know which of the three interpolation methods presented here closest resembles the real fields as they differ from each other (Figure 34). A next step would thus be to create an idealised data set to determine their accuracy. Heat and freshwater transports from interpolated temperature and salinity fields could then be compared to the known overall transport.

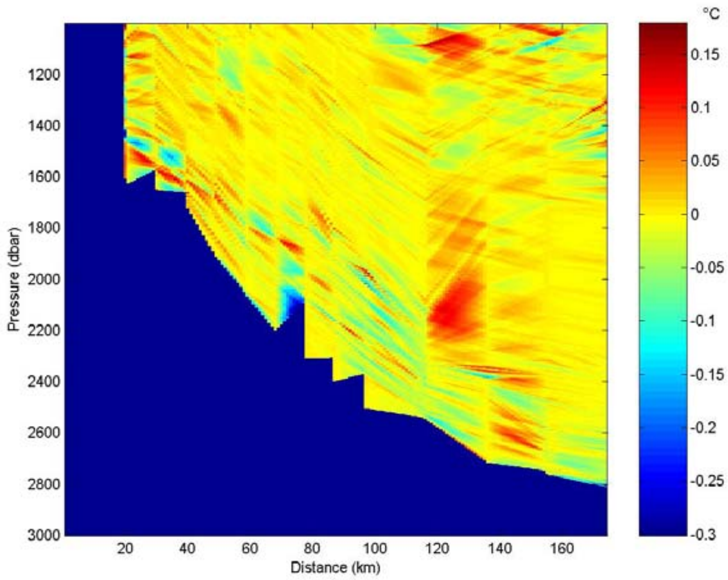

Figure 34: Difference between the temperature fields from interpolation with a flat bottom and interpolation along isopycnals for depths below 1000m

Meso-scale Eddies in the Denmark Strait Overflow plume
Data analysis of the UK1-05 mooring

Moorings are one particular fixed point method for measuring the Denmark Strait Overflow plume in the northern Atlantic. On September 23rd, 2006, during our cruise D311 we recovered the mooring UK1-05 at position 63° 29' N 36° 18' W, which had been deployed in August 2005. During this 13.5 month period three Seabird SBE 37 (microcats) measured continously conductivity and temperature at three different depth (top: 1595dBar = 1574m, middle: 1773dBar = 1748m, bottom: 1962dBar = 1933m). The two upper microcats also measured pressure.

The idea for this study was to identify meso-scale cold core eddies in the Denmark Strait Overflow plume by analysing the variability in the data set provided.
The theories that explain observed meso-scale eddies in the Denmark Strait Overflow is based on the physical mechanisms of vortex stretching and baroclinic instability. Eddies are formed as the dense water descends the slope from the sill (Figure 35). To conserve the potential vorticity of the water column while stretching it starts to spin cyclonically. The thickness in the dense water layer increases below the eddies and adopts a domelike.

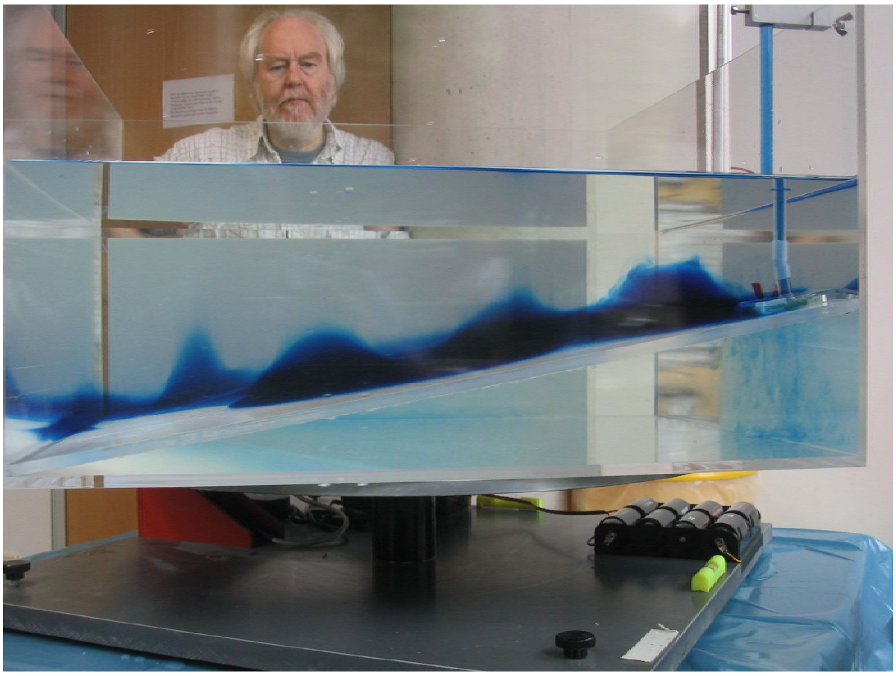

Figure 35: Tankexperiment – Dome shaped eddies

In accordance with Voet (2006) these meso-scale eddies have a timescale of 3-10 days. We expected to recognize the cold core eddies in our salinity, temperature and density signals.

The original data set consists of conductivity, temperature and pressure values taken every 10 over the whole period of 13.5 months. By examining the pressure data from the upper two instruments we realized that the mooring slid down the slope about ten meters after the first 38 days.

We calculated the bottom instrument's pressure by using its estimated depth and the variability from the upper levels, and included the change after 38 days (Figure 36). The high frequency variability in the pressure data is probably caused by the tides and internal waves.

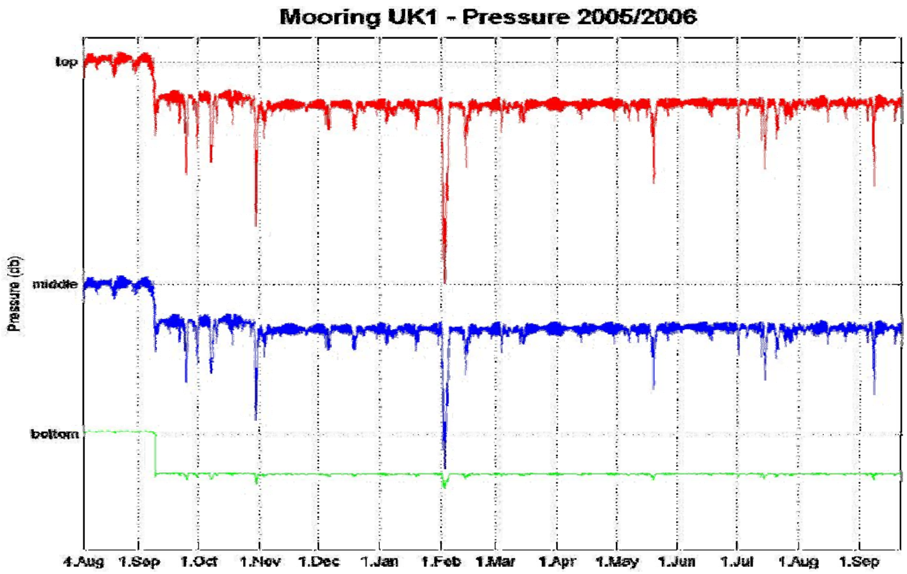

Figure 36: Mooring UK1 – Pressure 2005/2006

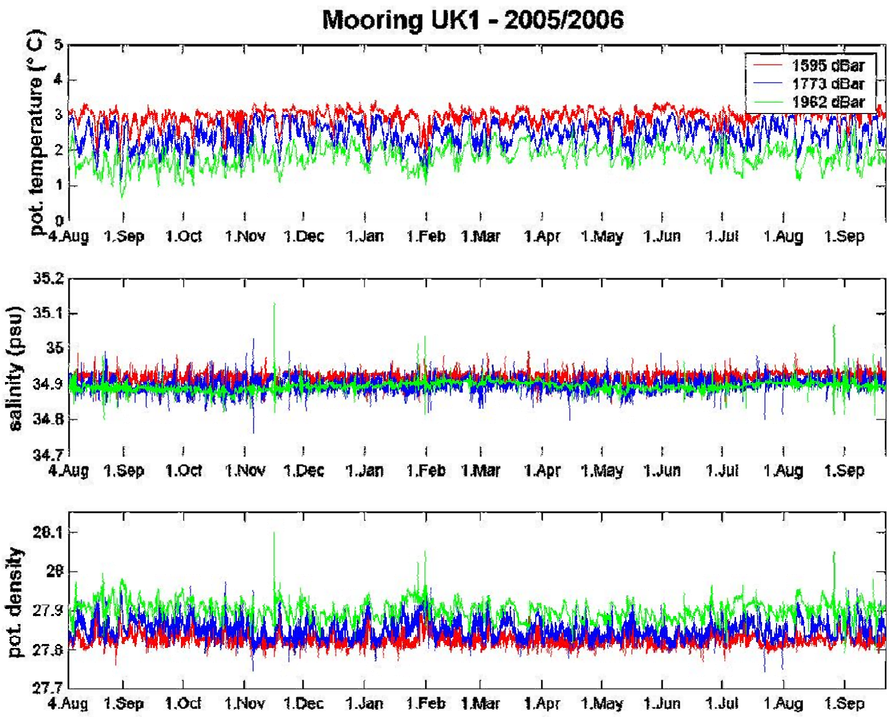

Figure 37: Mooring UK1 – pot. Temperature, Salinity, pot. Density

The large peaks (Oct, Nov, Feb,May,Jul, Sep) might be caused by higher current velocities knocking down the instruments. The vertical movement of the instruments shown by the pressure data also influences the temperature and conductivity values.

The next step was to compute salinity, potential temperature and potential density. To get a first impression of the variability range we created time plots of these parameters. (Figure 37). The mean potential densities are 27.8249 ± 0.0153 (top), 27.8526 ± 0.0230 (middle) and 27.9022 ± 0.0230 (bottom).

Figure 37 shows the expected strong high frequency variability in the data. When we compare these time series with Figure 36, we find a peak consistency with pressure peak values in all parameters (e.g. November and February).

The spectrum of the pressure signal given by discrete Fourier transformation of the top data (Figure 38) appears to confirm this suggestion. Figure 38 shows three peaks, the M1 tide, the M2 tide and the inertial period. For 63° 29' N the inertial period is 13.341 h. To extract the timescales of interest we used a bandpass filter. The filter cuts off the frequencies below 1/(15 days) and higher than 1/(36h). Figure 39 shows an example of the effect of the filter on the bottom salinity spectrum, while Figure 40 shows the unfiltered and the filtered data as a time-series.

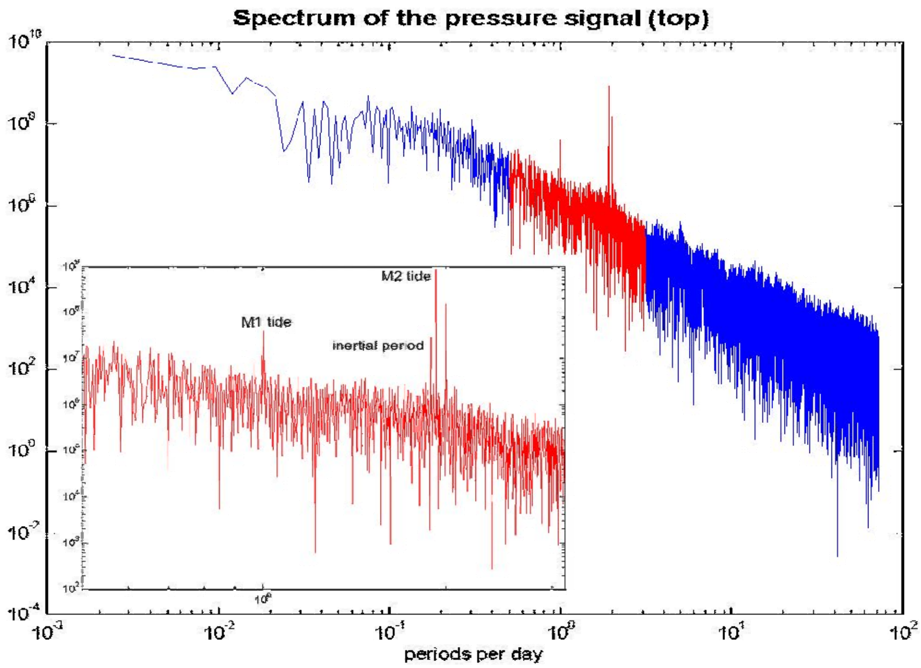

Figure 38: Mooring UK1 – Pressure 2005/2006

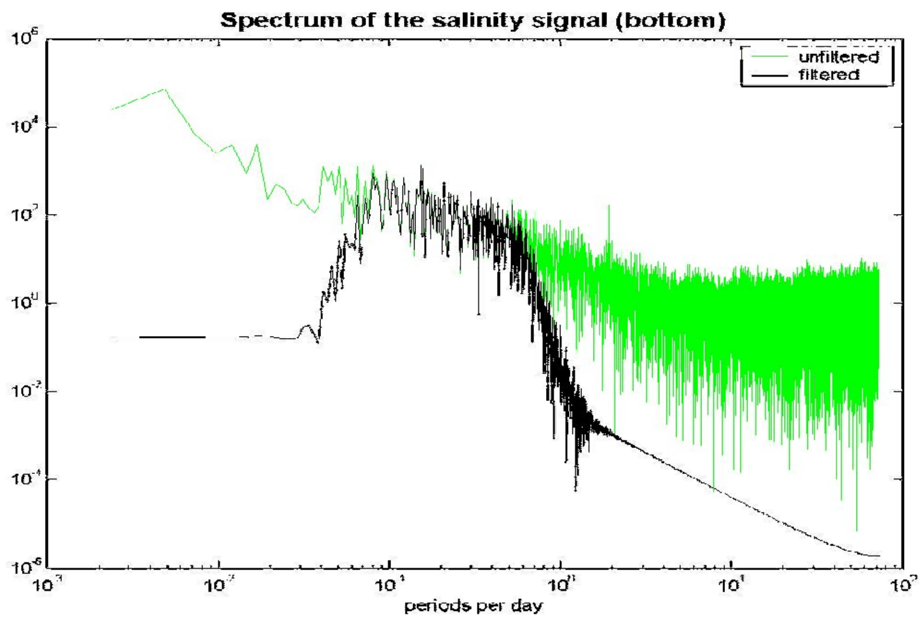

Figure 39: Spectrum of the salinity (bottom)

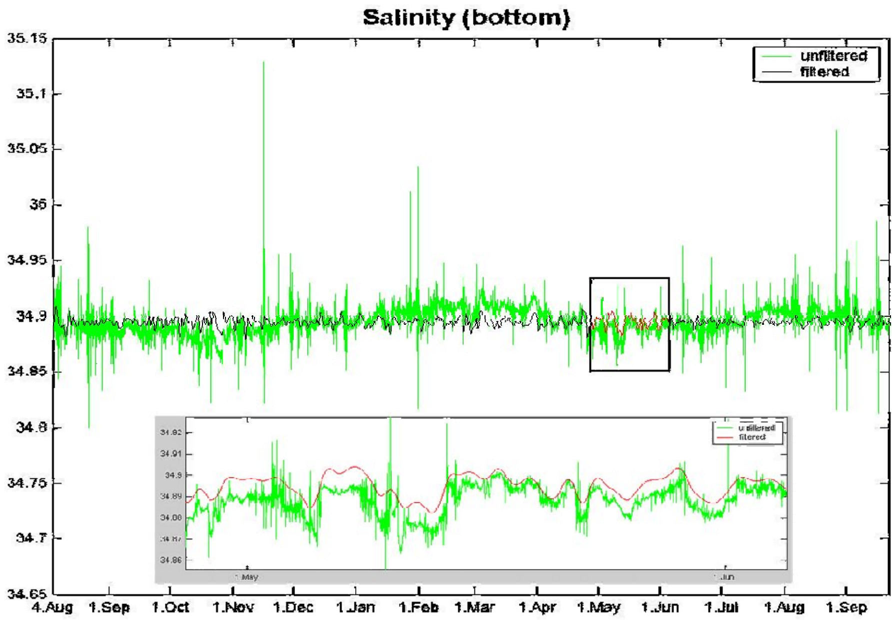

Figure 40: Salinity (bottom) – filtered, unfiltered

Then each parameter (potential temperature, salinity and potential density) was interpolated between the three depths in steps of 10 dBar. The filtering of our data made it possible to pick out every 18th value (three hour steps) without losing the signals of our interest. Afterwards we created contour plots for each parameter for the period of two months (Figures 41). We added the 27.85 isopycnal to each plot, which can be used to define an upper boundary for the overflow plume. In these contour plots, particularly in potential temperature, we can now identify about 3-4 cold core eddies per months in the Denmark Strait Overflow plume. The mean depth of the plume upper boundary is 1,710 m with a standard deviation of 60 m.

Finally we compared our results with CTD measurements at the position of UK1-05 from 1998 to 2003. We created a pressure/potential density plot from these CTD data and added three lines at the depths of the UK1-05 microcats and the mean potential densities plus standard deviations of the mooring measurements (Figure 42a). The CTD data sets of the different years show a high variability. Some data sets do not even fit in the range of the mooring mean data's standard deviations. So they can hardly be used for identifying cold core eddies.

Then we picked a single potential density value at the three UK1-05 depths out of each CTD data set and interpolated between these three. The result is shown in figure 41b. It gives an impression of the differences between original data (Figure 42a) and interpolated data (Figure 42b). There is a great loss of vertical spatial resolution by using only 3 depths points.

For both, vertical spatial and temporal high resolution of the measurements we suggest to deploy Jojo-moorings, which measure continuously in small depth and time intervals.

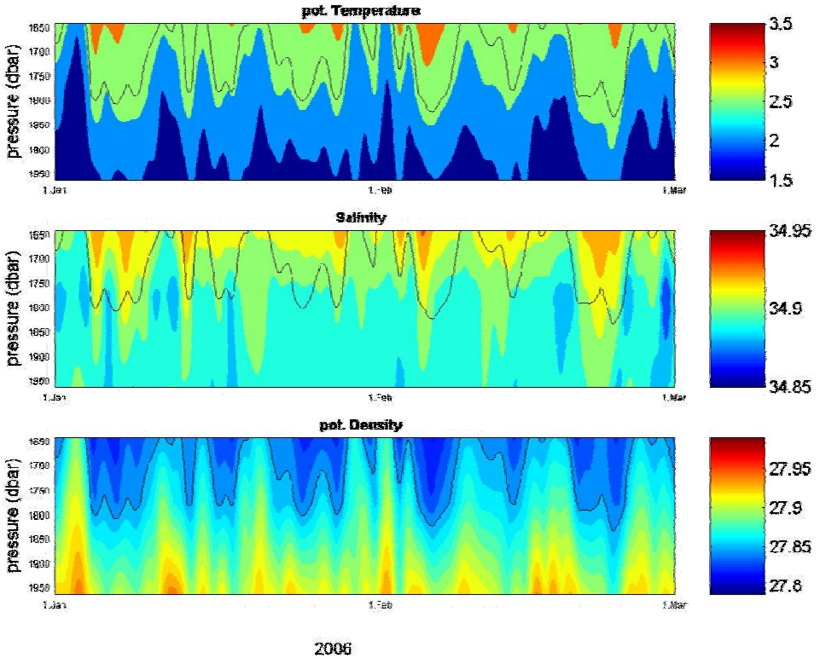

Figures 41(a, b, c): Contour plots - pot. Temperature, Salinity, pot. Density

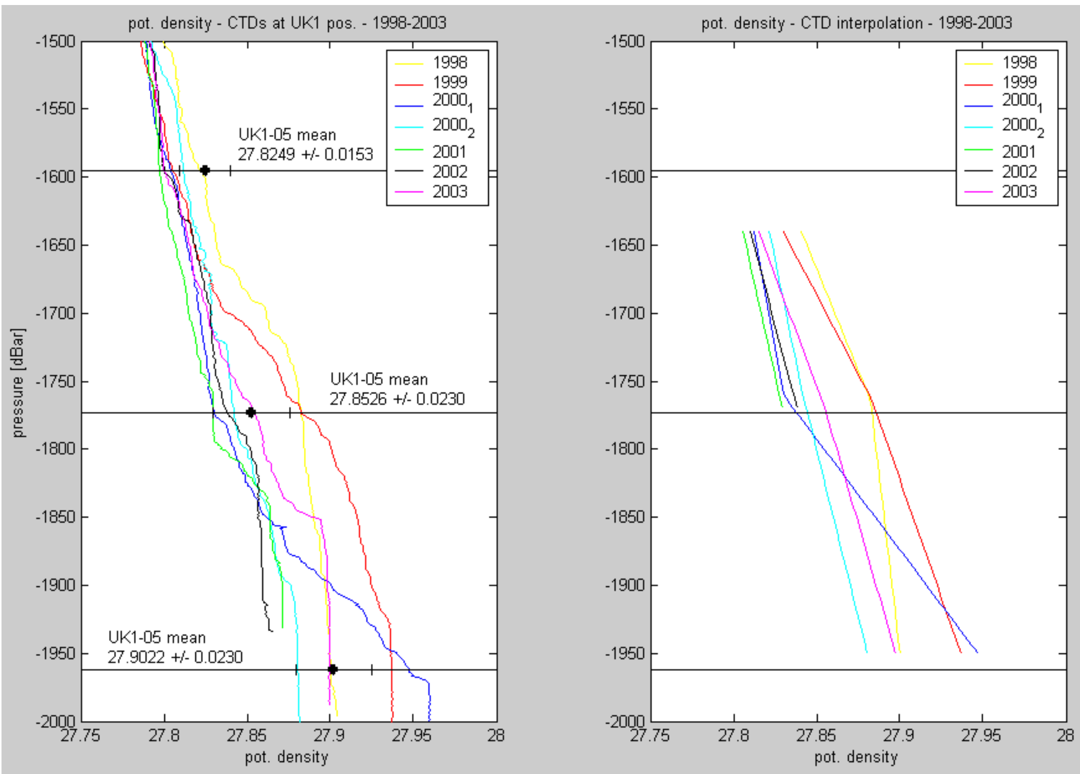

Figure 42 (a, b): CTD data at UK1 Position 1998-2003

7. Acknowledgements

We like to thank Captain Peter Sarjeant, his officers and crew of RRS DISCOVERY and the UKORS technical staff for their support of our measurement programme and for creating a very friendly atmosphere on board.

Financial support by the different funding agencies of the participating scientific groups is gratefully acknowledged.

Mooring recoveries:

DS-ADCP:	V425-04	66° 07.24' N	27° 16.19' W		580 m
		Released:	10.09.2006	13:50 Z	
		Not recovered			
ASOF:	G2-05	63° 07.19' N	35° 32.50' W		2545 m
		Released:	22.09.2006	07:50 Z	
		Not recovered			
ASOF:	UK2-05	63° 16.94' N	35° 52.24' W		2320 m
		Released:	22.09.2006	10:29 Z	
		On deck:		11:30 Z	
ASOF:	G1-05	63° 21.99' N	36° 04.20' W		2160 m
		Released:	22.09.2004	12:22 Z	
		On deck:		13:20 Z	
ASOF:	UK1-05	63° 29.07' N	36° 18.10' W		1954 m
		Released:	22.09.2006	14:29 Z	
		On deck:		15:37 Z	
ASOF:	F1/2-05	63° 35.48' N	36° 38.90' W		1687 m
		Released:	22.09.2006	16:52 Z	
		On deck:		17:42 Z	
ASOF:	ADCP-21	63° 01.12' N	40° 31.49' W		219 m
		Grappled:	23.09.2007	08:38 Z	
		On deck:		10:41 Z	
ASOF:	TUBE-21	63° 00.27' N	40° 32.75' W		295 m
		Released:	23.09.2006	12:38 Z	
		Not recovered			

Mooring deployments

ASOF:	TUBE-28	63° 00.22' N	40° 32.73' W		305 m
		Top Buoy in water:		23.09.2006	14:35 Z
		Anchor released:			15:22 Z
ASOF:	ADCP-28	63° 00.88' N	40° 31.22' W		218 m
		Anchor at bottom:		25.09.2006	11:35 Z
		63° 01.05' N	40° 30.95' W		205 m
		ADCP at bottom:		25.09.2006	12:16 Z
ASOF:	F1/2-06	63° 35.44' N	36° 39.26' W		1717 m
		Top Buoy in water:		26.09.2006	09:23 Z
		Anchor released:			10:22 Z
ASOF:	UK1-06	63° 29.01' N	36° 17.98' W		1988 m
		Top Buoy in water:		26.09.2006	13:15 Z
		Anchor released:			13:49 Z
ASOF:	G1-06	63° 22.10' N	36° 04.36' W		2158 m
		Top Buoy in water:		26.09.2006	15:43 Z
		Anchor released:			16:13 Z
ASOF:	UK2-06	63° 16.92' N	35° 52.09' W		2358 m
		Top Buoy in water:		26.09.2004	17:37 Z
		Anchor released:			18:06 Z

EXPO-CODE	Section Name	Discovery Stat. No.	Stat. No.	Cast No.	Cast Type	Date mmddyy	Time UTC	Code	Position Latitude	Longitude	Code	Bottom depth	Max Press.	meter wheel	Bottom Dist.	No. Of Bottles	Param.	Comments
74DI311_1	DS1	16024	001	001	ROS/CTD	090906	1512	BE	64 30.83 N	23 21.42 W	GPS	146						test
74DI311_1	DS1	16024	001	001	ROS/CTD	090906	1518	BO	64 30.87 N	23 21.31 W	GPS	146	135	130		14		
74DI311_1	DS1	16024	001	001	ROS/CTD	090906	1534	EN	64 30.88 N	23 21.15 W	GPS	145						
74DI311_1	DS1	16025	002	001	ROS/CTD	091006	0855	BE	66 00.17 N	26 44.68 W	GPS	288						Pumpe aus bei 100m
74DI311_1	DS1	16025	002	001	ROS/CTD	091006	0926	BO	66 00.28 N	26 44.19 W	GPS	380	361	360		1		
74DI311_1	DS1	16025	002	001	ROS/CTD	091006	0941	EN	66 00.30 N	26 43.82 W	GPS	?						
74DI311_1	DS1	16025	002	002	ROS/CTD	091006	1045	BE	66 59.98 N	26 44.87 W	GPS	380						
74DI311_1	DS1	16025	002	002	ROS/CTD	091006	1100	BO	66 00.01 N	26 44.70 W	GPS	368	352	350		1		
74DI311_1	DS1	16025	002	002	ROS/CTD	091006	1114	EN	66 00.11 N	26 44.50 W	GPS	372						
74DI311_1	DS1	16026	003	001	ROS/CTD	091006	1519	BE	66 07.34 N	27 16.87 W	GPS	580						
74DI311_1	DS1	16026	003	001	ROS/CTD	091006	1539	BO	66 07.30 N	27 17.75 W	GPS	565	555	550		12	1, 2, 7,	
74DI311_1	DS1	16026	003	001	ROS/CTD	091006	1618	EN	66 06.75 N	27 17.54 W	GPS	591					9, 10, 20	
74DI311_1	DS1	16027	004	001	ROS/CTD	091006	1931	BE	66 01.31 N	26 51.41 W	GPS	520						
74DI311_1	DS1	16027	004	001	ROS/CTD	091006	1944	BO	66 01.20 N	26 51.43 W	GPS	516	507	500		5		
74DI311_1	DS1	16027	004	001	ROS/CTD	091006	2007	EN	66 01.18 N	26 51.15 W	GPS	514					1, 2, 20	
74DI311_1	DS1	16028	005	001	ROS/CTD	091006	2124	BE	66 02.96 N	26 57.59 W	GPS	618						
74DI311_1	DS1	16028	005	001	ROS/CTD	091006	2147	BO	66 03.06 N	26 57.42 W	GPS	618	578	570		12	1, 2, 7,	
74DI311_1	DS1	16028	005	001	ROS/CTD	091006	2225	EN	66 03.05 N	26 56.91 W	GPS	613					9, 10, 20	
74DI311_1	DS1	16029	006	001	ROS/CTD	091106	0038	BE	66 04.66 N	27 03.66 W	GPS	673						aborted sensor failure, cast abandoned because
74DI311_1	DS1	16029			ROS/CTD			BO			GPS					0		of noisy temperature and conductivity signals
74DI311_1	DS1	16029	006	001	ROS/CTD	091106	0109	EN	66 04.57 N	27 03.02 W	GPS	667						started at 200m, CDT stopped at 340 m
74DI311_1	DS1	16029	006	002	ROS/CTD	091106	0322	BE	66 04.31 N	27 04.25 W	GPS	676						
74DI311_1	DS1	16029	006	002	ROS/CTD	091106	0344	BO	66 03.94 N	27 04.11 W	GPS	669	642	640		5		
74DI311_1	DS1	16029	006	002	ROS/CTD	091106	0412	EN	66 03.46 N	27 04.25 W	GPS	659					1, 2, 20	
74DI311_1	DS1	16030	007	001	ROS/CTD	091106	0552	BE	66 05.90 N	27 10.58 W	GPS	636						at 480m conductivity sensor dirty
74DI311_1	DS1	16030	007	001	ROS/CTD	091106	0612	BO	66 05.41 N	27 11.20 W	GPS	645	612	610		12	1, 2, 7,	
74DI311_1	DS1	16030	007	001	ROS/CTD	091106	0647	EN	66 04.83 N	27 11.90 W	GPS	652					9, 10, 20	
74DI311_1	DS1	16031	008	001	ROS/CTD	091106	0846	BE	66 09.04 N	27 22.70 W	GPS	506						
74DI311_1	DS1	16031	008	001	ROS/CTD	091106	0911	BO	66 09.03 N	27 22.59 W	GPS	505	485	480		3		
74DI311_1	DS1	16031	008	001	ROS/CTD	091106	0931	EN	66 08.93 N	27 22.57 W	GPS	506					1	
74DI311_1	DS1	16032	009	001	ROS/CTD	091106	1037	BE	66 10.54 N	27 29.12 W	GPS	501						
74DI311_1	DS1	16032	009	001	ROS/CTD	091106	1054	BO	66 10.58 N	27 29.06 W	GPS	500	483	475		12	1, 2, 7,	
74DI311_1	DS1	16032	009	001	ROS/CTD	091106	1123	EN	66 10.61 N	27 29.02 W	GPS	501					9, 10, 20	

1: Salinity
7: CFC
10: Helium

2: Oxygen
9: Tritium
20: O18

EXPO-CODE	Section Name	Discovery Stat. No.	Stat. No.	Cast No.	Cast Type	Date mmddyy	Time UTC	Code	Position Latitude	Position Longitude	Code	Bottom depth	Max Press.	meter wheel	Bottom Dist.	No. Of Bottles	Param.	Comments
74DI311_1	DS1	16033	010	001	ROS/CTD	091106	1308	BE	66 12.28 N	27 35.35 W	GPS	500						
74DI311_1	DS1	16033	010	001	ROS/CTD	091106	1325	BO	66 12.29 N	27 35.68 W	GPS	501	484	475		4		
74DI311_1	DS1	16033	010	001	ROS/CTD	091106	1348	EN	66 12.55 N	27 35.57 W	GPS	501					1, 20	
74DI311_1	DS1	16034	011	001	ROS/CTD	091106	1517	BE	66 16.14 N	27 50.39 W	GPS	468						
74DI311_1	DS1	16034	011	001	ROS/CTD	091106	1534	BO	66 16.25 N	27 50.66 W	GPS	470	449	440		12	1, 2, 7,	
74DI311_1	DS1	16034	011	001	ROS/CTD	091106	1607	EN	66 16.07 N	27 51.55 W	GPS	464					9, 10, 20	
74DI311_1	DS1	16035	012	001	ROS/CTD	091106	1816	BE	66 19.69 N	28 05.82 W	GPS	350						Header file: wrong time
74DI311_1	DS1	16035	012	001	ROS/CTD	091106	1831	BO	66 19.55 N	28 06.16 W	GPS	350	332	325		5		
74DI311_1	DS1	16035	012	001	ROS/CTD	091106	1852	EN	66 19.33 N	28 06.77 W	GPS	352					1, 2, 20	
74DI311_1	DS1	16036	013	001	ROS/CTD	091106	2109	BE	66 23.92 N	28 21.09 W	GPS	338						
74DI311_1	DS1	16036	013	001	ROS/CTD	091106	2122	BO	66 23.86 N	28 21.25 W	GPS	338	316	310		3		
74DI311_1	DS1	16036	013	001	ROS/CTD	091106	2138	EN	66 23.88 N	28 21.39 W	GPS	334					1, 2, 20	
74DI311_1	DS1	16037	014	001	ROS/CTD	091106	2332	BE	66 28.14 N	28 34.95 W	GPS	330						
74DI311_1	DS1	16037	014	001	ROS/CTD	091106	2345	BO	66 28.10 N	28 34.66 W	GPS	331	312	305		3		
74DI311_1	DS1	16037	014	001	ROS/CTD	091106	2358	EN	66 28.16 N	28 34.38 W	GPS	328					1, 2, 20	
74DI311_1	DS1	16038	015	001	ROS/CTD	091206	0127	BE	66 32.34 N	28 50.05 W	GPS	329						
74DI311_1	DS1	16038	015	001	ROS/CTD	091206	0140	BO	66 32.42 N	28 50.95 W	GPS	316	317	310		3		
74DI311_1	DS1	16038	015	001	ROS/CTD	091206	0155	EN	66 32.48 N	28 49.74 W	GPS	329					1, 2, 20	
74DI311_1	DS1	16039	016	001	ROS/CTD	091206	0320	BE	66 36.51 N	29 05.45 W	GPS	324						
74DI311_1	DS1	16039	016	001	ROS/CTD	091206	0332	BO	66 36.54 N	29 05.34 W	GPS	323	315	310		10	1, 2, 7,	
74DI311_1	DS1	16039	016	001	ROS/CTD	091206	0402	EN	66 36.58 N	29 04.89 W	GPS	324					9, 10, 20	
74DI311_1	DS2	16040	017	001	ROS/CTD	091206	2141	BE	67 09.96 N	22 40.23 W	GPS	309						
74DI311_1	DS2	16040	017	001	ROS/CTD	091206	2154	BO	67 09.95 N	22 40.28 W	GPS	309	292	285		9	1, 2, 7,	
74DI311_1	DS2	16040	017	001	ROS/CTD	091206	2213	EN	67 09.97 N	22 40.17 W	GPS	308					9, 10, 20	
74DI311_1	DS2	16041	018	001	ROS/CTD	091206	2355	BE	67 15.96 N	22 40.16 W	GPS	341						
74DI311_1	DS2	16041	018	001	ROS/CTD	091306	0007	BO	67 15.97 N	22 40.03 W	GPS	342	326	320		4		
74DI311_1	DS2	16041	018	001	ROS/CTD	091306	0023	EN	67 15.98 N	22 39.99 W	GPS	342					1, 2	
74DI311_1	DS2	16042	019	001	ROS/CTD	091306	0155	BE	67 21.76 N	22 40.63 W	GPS	391						cable out 364m, altimeter 12 m
74DI311_1	DS2	16042	019	001	ROS/CTD	091306	0206	BO	67 21.65 N	22 40.62 W	GPS	642	370,6	364		3		
74DI311_1	DS2	16042	019	001	ROS/CTD	091306	0220	EN	67 21.70 N	22 40.53 W	GPS	388					1, 2	
74DI311_1	DS2	16043	020	001	ROS/CTD	091606	1528	BE	67 28.05 N	22 39.63 W	GPS	502						
74DI311_1	DS2	16043	020	001	ROS/CTD	091606	1533	BO	67 28.10 N	22 39.50 W	GPS	512	482	475	10	3		
74DI311_1	DS2	16043	020	001	ROS/CTD	091606	1540	EN	67 28.12 N	22 39.30 W	GPS	497					1, 2	

1: Salinity
7: CFC
10: Helium

2: Oxygen
9: Tritium
20: O18

EXPO-CODE	Section Name	Discovery Stat. No.	Stat. No.	Cast No.	Cast Type	Date mmddyy	Time UTC	Code	Position Latitude	Longitude	Code	Bottom depth	Max Press.	meter wheel	Bottom Dist.	No. Of Bottles	Param.	Comments
74DI311_1	DS2	16044	021	001	ROS/CTD	091606	1657	BE	67 34.03 N	22 39.77 W	GPS	599						
74DI311_1	DS2	16044	021	001	ROS/CTD	091606	1713	BO	67 33.94 N	22 39.68 W	GPS	580	575	569	9.4	10	1, 2, 7,	
74DI311_1	DS2	16044	021	001	ROS/CTD	091606	1745	EN	67 33.80	22 39.26 W	GPS	592					9, 10, 20	
74DI311_1	DS2	16045	022	001	ROS/CTD	091606	1914	BE	67 39.96 N	22 40.27 W	GPS	684						
74DI311_1	DS2	16045	022	001	ROS/CTD	091606	1932	BO	67 39.91 N	22 40.71 W	GPS	666	657	655	9.9	4		
74DI311_1	DS2	16045	022	001	ROS/CTD	091606	1957	EN	67 40.02 N	22 41.02 W	GPS	685					1, 2	
74DI311_1	DS2	16046	023	001	ROS/CTD	091606	2107	BE	67 45.95 N	22 40.48 W	GPS	757						
74DI311_1	DS2	16046	023	001	ROS/CTD	091606	2126	BO	67 46.06 N	22 41.01 W	GPS		739	730	7.8	11	1, 2, 7,	
74DI311_1	DS2	16046	023	001	ROS/CTD	091606	2201	EN	67 46.26 N	22 41.54 W	GPS	665					9, 10, 20	
74DI311_1	DS2	16047	024	001	ROS/CTD	091606	2335	BE	67 51.92 N	22 39.99 W	GPS	876						
74DI311_1	DS2	16047	024	001	ROS/CTD	091606	2353	BO	67 52.19 N	22 40.19 W	GPS	857	846	845	12.2	5		
74DI311_1	DS2	16047	024	001	ROS/CTD	091706	0025	EN	67 52.38 N	22 40.38 W	GPS	895					1, 2	
74DI311_1	DS2	16048	025	001	ROS/CTD	091706	0140	BE	67 57.90 N	22 39.89 W	GPS	1069						
74DI311_1	DS2	16048	025	001	ROS/CTD	091706	0204	BO	67 58.02 N	22 39.34 W	GPS	1070	1046	1040	10.0	5		
74DI311_1	DS2	16048	025	001	ROS/CTD	091706	0242	EN	67 58.12 N	22 38.61 W	GPS	1062					1, 2	
74DI311_1	DS2	16049	026	001	ROS/CTD	091706	0409	BE	68 03.88 N	22 39.85 W	GPS	n.a.						
74DI311_1	DS2	16049	026	001	ROS/CTD	091706	0437	BO	68 03.92 N	22 39.75 W	GPS	1015	1046	1040	10.0	5		
74DI311_1	DS2	16049	026	001	ROS/CTD	091706	0510	EN	68 03.99 N	22 39.90 W	GPS	n.a.					1, 2	
74DI311_1	DS2	16050	027	001	ROS/CTD	091706	0655	BE	68 16.02 N	22 40.03 W	GPS	1301						
74DI311_1	DS2	16050	027	001	ROS/CTD	091706	0725	BO	68 16.15 N	22 40.28 W	GPS	1300	1305	1290	9.6	5		
74DI311_1	DS2	16050	027	001	ROS/CTD	091706	0758	EN	68 16.35 N	22 40.51 W	GPS	n.a.					1, 2	
74DI311_1	DS2	16051	028	001	ROS/CTD	091706	0937	BE	68 28.01 N	22 40.36 W	GPS	1459						
74DI311_1	DS2	16051	028	001	ROS/CTD	091706	1009	BO	68 28.32 N	22 41.11 W	GPS	1422	1434	1422	10.4	13	1, 2, 7,	
74DI311_1	DS2	16051	028	001	ROS/CTD	091706	1055	EN	68 28.65 N	22 41.95 W	GPS	1469					9, 10, 20	
74DI311_1	DS2	16052	029	001	ROS/CTD	091706	1241	BE	68 35.91 N	23 06.14 W	GPS	1529						
74DI311_1	DS2	16052	029	001	ROS/CTD	091706	1313	BO	68 35.62 N	23 06.96 W	GPS	1527	1498	1480	11	13	1, 2, 7,	
74DI311_1	DS2	16052	029	001	ROS/CTD	091706	1356	EN	68 35.23 N	23 07.91 W	GPS	1527					9, 10, 20	
74DI311_1	DS2	16053	030	001	ROS/CTD	091706	1532	BE	68 39.98 N	23 19.06 W	GPS	1401						
74DI311_1	DS2	16053	030	001	ROS/CTD	091706	1601	BO	68 39.64 N	23 19.68 W	GPS	1415	1340.4	1370	21	12		
74DI311_1	DS2	16053	030	001	ROS/CTD	091706	1647	EN	68 39.40 N	23 19.99 W	GPS	1422					1, 2, 20	
74DI311_1	DS2	16054	031	001	ROS/CTD	091706	1800	BE	68 43.99 N	23 32.21 W	GPS	537						
74DI311_1	DS2	16054	031	001	ROS/CTD	091706	1812	BO	68 43.87 N	23 32.69 W	GPS	532	516.7	510	12.6	9	1, 2, 7,	
74DI311_1	DS2	16054	031	001	ROS/CTD	091706	1842	EN	68 43.70 N	23 33.20 W	GPS	529					9, 10, 20	
74DI311_1	DS2	16055	032	001	ROS/CTD	091706	2015	BE	68 48.02 N	23 45.76 W	GPS	322						

1: Salinity
7: CFC
10: Helium

2: Oxygen
9: Tritium
20: O18

EXPO-	Section	Discovery	Stat.	Cast	Cast	Date	Time		Position			Bottom	Max	meter	Bottom	No. Of	Param.	Comments
CODE	Name	Stat. No.	No.	No.	Type	mmddyy	UTC	Code	Latitude	Longitude	Code	depth	Press.	wheel	Dist.	Bottles		
74DI311_1	DS2	16055	032	001	ROS/CTD	091706	2029	BO	68 48.16 N	23 45.87 W	GPS	321	304	300	7.2	13		
74DI311_1	DS2	16055	032	001	ROS/CTD	091706	2049	EN	68 48.41 N	23 45.16 W	GPS	324					1, 2, 20	
74DI311_1	DS2	16056	033	001	UNK	091906	0915	BE	64 39.9 N	23 14.2 W	GPS							test ROV
74DI311_1	DS2	16056	033	001	UNK	091906	1433	EN	64 39.5 N	23 11.9 W	GPS							
74DI311_2	DS3	16057	034	001	CTD	092106	1600	BE	63 22.4 N	31 27.3 W	GPS							Microstructure Test run
74DI311_2	DS3	16057	034	001	CTD	092106	1650	EN	63 23.1 N	31 27.9 W	GPS							postponed
74DI311_2	DS3	16058	035	001	MOR	092206			63 07.19 N	35 32.50 W	GPS	2545						nom. Pos.
74DI311_2	DS3	16058	035	001	MOR	092206	0712	BE	63 07.0 N	35 33.1 W	GPS							Recovery of mooring G2-05 failed
74DI311_2	DS3	16058	035	001	MOR	092206	0900	EN	63 07.4 N	35 32.6 W	GPS							
74DI311_2	DS3	16059	036	001	MOR	092206			63 16.94 N	35 52.24 W	GPS	2320						nom. Pos.
74DI311_2	DS3	16059	036	001	MOR	092206	1026	BE	63 16.7 N	35 52.5 W	GPS							Recovery of Mooring UK2-05
74DI311_2	DS3	16059	036	001	MOR	092206	1125	EN	63 17.3 N	35 52.6 W	GPS							
74DI311_2	DS3	16060	037	001	MOR	092206			63 21.99 N	36 04.20 W	GPS	2160						nom. Pos.
74DI311_2	DS3	16060	037	001	MOR	092206	1220	BE	63 21.7 N	35 03.8 W	GPS							Recovery of Mooring G1-05
74DI311_2	DS3	16060	037	001	MOR	092206	1322	EN	63 22.0 N	35 04.2 W	GPS							

1: Salinity
7: CFC
10: Helium

2: Oxygen
9: Tritium
20: O18

EXPO-	Section	Discovery	Stat.	Cast	Cast	Date	Time		Position			Bottom	Max	meter	Bottom	No. Of	Param.	Comments
CODE	Name	Stat. No.	No.	No.	Type	mmddyy	UTC	Code	Latitude	Longitude	Code	depth	Press.	wheel	Dist.	Bottles		
74DI311_2	DS3	16061	038	001	MOR	092206			63 29.07 N	36 18.10 W	GPS	1954						nom. Pos.
74DI311_2	DS3	16061	038	001	MOR	092206	1425	BE	63 28.7 N	36 17.9 W	GPS							Recovery of Mooring UK1-05
74DI311_2	DS3	16061	038	001	MOR	092206	1537	EN	63 29.1 N	36 19.5 W	GPS							
74DI311_2	DS3	16062	039	001	MOR	092206			63 35.48 N	36 38.90 W	GPS	1687						nom. Pos.
74DI311_2	DS3	16062	039	001	MOR	092206	1649	BE	63 35.2 N	36 38.7 W	GPS							Recovery of Mooring F12-05
74DI311_2	DS3	16062	039	001	MOR	092206	1742	EN	63 35.7 N	36 39.8 W	GPS							
74DI311_2	DS4	16063	040	001	MOR	092306			63 01.12 N	40 31.5 W	GPS	219						nom. Pos.
74DI311_2	DS4	16063	040	001	MOR	092306	0735	BE	63 01.0 N	40 31.8 W	GPS							mooring ADCP Recovered
74DI311_2	DS4	16063	040	001	MOR	092306	1041	EN	63 00.8 N	40 31.4 W	GPS							
74DI311_2	DS4	16064	041	001	MOR	092306			63 00.27 N	40 32.75 W	GPS	295						nom. Pos.
74DI311_2	DS4	16064	041	001	MOR	092306	1102	BE	63 00.4 N	40 32.2 W	GPS							Recovery of mooring TUBE-21 failed
74DI311_2	DS4	16064	041	001	MOR	092306	1238	EN	63 00.2 N	40 33.4 W	GPS							
74DI311_2	DS4	16065	042	001	MOR	092306	1433	BE	63 00.78 N	40 31.32 W	GPS	223						mooring TUBE-28 deployed
74DI311_2	DS4	16065	042	001	MOR	092306	1521	EN	63 00.21 N	40 32.73 W	GPS	305						released
74DI311_2	DS4	16066	043	001	ROS/CTD	092306	1716	BE	63 10.5 N	41 01.08 W	GPS	224						
74DI311_2	DS4	16066	043	001	ROS/CTD	092306	1730	BO	63 10.0 N	41 01.19 W	GPS	233	229	225	12	5	1,2,7,9,	
74DI311_2	DS3	16066	043	001	ROS/CTD	092306	1746	EN	63 01.31 N	41 01.31 W	GPS	191					10,20	
74DI311_2	DS4	16067	044	001	ROS/CTD	092306	1849	BE	63 06.96 N	40 52.25 W	GPS	290						
74DI311_2	DS4	16067	044	001	ROS/CTD	092306	1859	BO	63 06.81 N	40 52.86 W	GPS		203	200	16	5		
74DI311_2	DS4	16067	044	001	ROS/CTD	092306	1914	EN	63 06.85 N	40 53.35 W	GPS	185					20	
74DI311_2	DS4	16068	045	001	ROS/CTD	092306	2047	BE	63 04.00 N	40 43.07 W	GPS	235						
74DI311_2	DS4	16068	045	001	ROS/CTD	092306	2102	BO	63 04.00 N	40 43.60 W	GPS	270	254	250	40	5		
74DI311_2	DS4	16068	045	001	ROS/CTD	092306	2117	EN	63 03.99 N	40 44.03 W	GPS	234					20	
74DI311_2	DS4	16069	046	001	ROS/CTD	092306	2232	BE	63 00.84 N	40 33.98 W	GPS	304						
74DI311_2	DS4	16069	046	001	ROS/CTD	092306	2245	BO	63 00.62 N	40 34.50 W	GPS	328	312	310	17	5		
74DI311_2	DS4	16069	046	001	ROS/CTD	092306	2303	EN	63 00.55 N	40 35.26 W	GPS	378					20	
74DI311_2	DS4	16070	047	001	ROS/CTD	092406	0024	BE	62 57.94 N	40 25.52 W	GPS	216						
74DI311_2	DS4	16070	047	001	ROS/CTD	092406	0036	BO	62 57.86 N	40 25.81 W	GPS	240	229	225	18	5		
74DI311_2	DS4	16070	047	001	ROS/CTD	092406	0052	EN	62 57.00 N	40 26.00 W	GPS	288					20	
74DI311_2	DS4	16071	048	001	ROS/CTD	092406	0216	BE	62 54.93 N	40 16.18 W	GPS	1305						
74DI311_2	DS4	16071	048	001	ROS/CTD	092406	0244	BO	62 54.74 N	40 16.42 W	GPS	1297	1282	1280	17	10	1,2,7,9,	
74DI311_2	DS4	16071	048	001	ROS/CTD	092406	0321	EN	62 54.66 N	40 16.94 W	GPS	1140					10,20	
74DI311_2	DS4	16072	049	001	ADCP	092506	1124	BE	63 00.86 N	40 31.25 W	GPS							
74DI311_2	DS4	16072	049	001	ADCP	092506	1135	BO	63 00.86 N	40 31.23 W	GPS	218						ADCP deployed
74DI311_2	DS4	16072	049	001	ADCP	092506	1216	EN	63 01.04 N	40 31.14 W	GPS	205						released
74DI311_2	DS4	16073	050	001	ROS/CTD	092506	1507	BE	63 01.93 N	39 57.77 W	GPS	1560						
74DI311_2	DS4	16073	050	001	ROS/CTD	092506	1538	BO	63 01.70 N	39 57.96 W	GPS	1540	1548	1525	15	5		
74DI311_2	DS4	16073	050	001	ROS/CTD	092506	1634	EN	63 01.82 N	39 58.67 W	GPS	1505					1	

1: Salinity
7: CFC
10: Helium

2: Oxygen
9: Tritium
20: O18

EXPO-	Section	Discovery	Stat.	Cast	Cast	Date	Time		Position			Bottom	Max	meter	Bottom	No. Of	Param.	Comments
CODE	Name	Stat. No.	No.	No.	Type	mmddyy	UTC	Code	Latitude	Longitude	Code	depth	Press.	wheel	Dist.	Bottles		
74DI311_2	DS4	16073	050	002		092506	1654	BE	63 01.6 N	39 59.0 W	GPS							
74DI311_2	DS4	16073	050	002		092506	1905	EN	63 00.2 N	40 00.2 W	GPS							Glider last signal given back
74DI311_2	DS4	16074	051	001	MOR	092606	0925	BE	63 35.43 N	36 39.58 W	GPS							Mooring F1-2 deployed
74DI311_2	DS4	16074	051	001	MOR	092606	1022	EN	63 35.48 N	36 17.97 W	GPS	1717						released
74DI311_2	DS4	16075	052	001	MOR	092606	1250	BE	63 28.97 N	36 18.35 W	GPS							Mooring UK1 deployed
74DI311_2	DS4	16075	052	001	MOR	092606	1349	EN	63 28.09 N	36 17.97 W	GPS	1982						released
74DI311_2	DS4	16076	053	001	MOR	092606	1542	BE	63 22.05 N	36 04.36 W	GPS							Mooring G1 deployed
74DI311_2	DS4	16076	053	001	MOR	092606	1612	EN	63 22.10 N	36 04.36 W	GPS	2160						released
74DI311_2	DS4	16077	054	001	MOR	092606	1734	BE	63 16.82 N	35 52.77 W	GPS							Mooring UK2 deployed
74DI311_2	DS4	16077	054	001	MOR	092606	1805	EN	63 16.91 N	35 52.09 W	GPS							released
74DI311_2	DS4	16078	055	001	ROS/CTD	092606	2207	BE	63 02.01 N	35 29.15 W	GPS	2648						LADCP Measurement
74DI311_2	DS4	16078	055	001	ROS/CTD	092606	2301	BO	63 01.87 N	35 28.99 W	GPS	2650	2661	2616	9.6	12	1,2,7,9,	
74DI311_2	DS4	16078	055	001	ROS/CTD	092606	0007	EN	63 01.98 N	35 28.82 W	GPS	2649					10,20	
74DI311_2	DS4	16079	056	001	ROS/CTD	092706	0717	BE	63 10.00 N	35 44.01 W	GPS	2501						LADCP Measurement
74DI311_2	DS4	16079	056	001	ROS/CTD	092706	0806	BO	63 10.15 N	35 44.34 W	GPS	2498	2502	2470	11.8	10		
74DI311_2	DS4	16079	056	001	ROS/CTD	092706	0908	EN	63 10.34 N	35 45.20 W	GPS	2490					1, 2, 20	
74DI311_2	DS4	16080	057	001	ROS/CTD	092706	1025	BE	63 14.08 N	35 51.23 W	GPS	2407						LADCP Measurement
74DI311_2	DS4	16080	057	001	ROS/CTD	092706	1117	BO	63 14.14 N	35 51.40 W	GPS	2405	2400	2370	15.0	9	1,2,7,9,	
74DI311_2	DS4	16080	057	001	ROS/CTD	092706	1212	EN	63 14.20 N	35 51.32 W	GPS	2403					10,20	
74DI311_2	DS4	16080	057	002	CTD	092706	1749	BE	65 30.06 N	31 10.06 W	GPS		101					Microstructure Test run
74DI311_2	DS4	16080	057	002	CTD	092706	1804	EN	65 30.24 N	31 11.08 W	GPS							
74DI311_2	DS	16081	058	001	ROS/CTD	092906	1839	BE	65 30.02 N	31 09.66 W	GPS	371						
74DI311_2	DS	16081	058	001	ROS/CTD	092906	1854	BO	65 29.98 N	31 10.09 W	GPS	375					1,2,7,9,	
74DI311_2	DS	16081	058	001	ROS/CTD	092906	1912	EN	65 29.99 N	31 10.90 W	GPS	370	372		8	7	10,20	
74DI311_2	DS	16082	059	001	ROS/CTD	092906	2057	BE	65 25.00 N	31 05.40 W	GPS	668						LADCP Measurement
74DI311_2	DS	16082	059	001	ROS/CTD	092906	2118	BO	65 25.13 N	31 06.09 W	GPS	660	654	650	11.1	9	1,2,7,9,	
74DI311_2	DS	16082	059	001	ROS/CTD	092906	2144	EN	65 25.25 N	31 07.29 W	GPS	651					10,20	
74DI311_2	DS	16083	060	001	ROS/CTD	092906	2321	BE	65 20.00 N	31 00.38 W	GPS	975						LADCP Measurement
74DI311_2	DS	16083	060	001	ROS/CTD	092906	2345	BO	65 20.22 N	31 01.51 W	GPS	970	967	960	10.0	11	1,2,7,9,	
74DI311_2	DS	16083	060	001	ROS/CTD	092906	0020	EN	65 20.39 N	31 04.31 W	GPS	957					10,20	
74DI311_2	DS	16084	061	001	ROS/CTD	093006	0138	BE	65 15.12 N	30 54.34 W	GPS	1248						LADCP Measurement
74DI311_2	DS	16084	061	001	ROS/CTD	093006	0202	BO	65 15.37 N	30 54.92 W	GPS	1210	1216	1200	7.6	12	1,2,7,9,	
74DI311_2	DS	16084	061	001	ROS/CTD	093006	0237	EN	65 15.98 N	30 55.70 W	GPS	1186					10,20	
74DI311_2	DS	16085	062	001	ROS/CTD	093006	0335	BE	65 09.92 N	30 50.00 W	GPS	1518						LADCP Measurement
74DI311_2	DS	16085	062	001	ROS/CTD	093006	0406	BO	65 10.23 N	30 50.60 W	GPS	1499	1491	1470	10.8	13	1,2,7,9,	
74DI311_2	DS	16085	062	001	ROS/CTD	093006	0452	EN	65 10.67 N	30 51.38 W	GPS	1468					10,20	

1: Salinity
7: CFC
10: Helium

2: Oxygen
9: Tritium
20: O18

EXPO-CODE	Section Name	Discovery Stat. No.	Stat. No.	Cast No.	Cast Type	Date mmddyy	Time UTC	Code	Position Latitude	Position Longitude	Code	Bottom depth	Max Press.	meter wheel	Bottom Dist.	No. Of Bottles	Param.	Comments
74DI311_2	DS	16086	063	001	ROS/CTD	093006	0602	BE	65 05.00 N	30 45.19 W	GPS	1761						LADCP Measurement
74DI311_2	DS	16086	063	001	ROS/CTD	093006	0636	BO	65 05.10 N	30 45.69 W	GPS	1757	1751	1725	11	13	1,2,7,9,	
74DI311_2	DS	16086	063	001	ROS/CTD	093006	0726	EN	65 05.42 N	30 46.18 W	GPS	1740					10,20	
74DI311_2	DS	16087	064	001	ROS/CTD	093006	0832	BE	64 59.99 N	30 40.16 W	GPS	1895						LADCP Measurement
74DI311_2	DS	16087	064	001	ROS/CTD	093006	0911	BO	65 00.12 N	30 40.90 W	GPS	1892	1892	1863	9.1	13	1,2,7,9,	
74DI311_2	DS	16087	064	001	ROS/CTD	093006	1005	EN	65 00.45 N	30 41.86 W	GPS	1892					10,20	
74DI311_2	DS	16088	065	001	ROS/CTD	093006	1131	BE	64 54.97 N	30 34.90 W	GPS	2037						LADCP Measurement
74DI311_2	DS	16088	065	001	ROS/CTD	093006	1214	BO	64 55.32 N	30 35.63 W	GPS	2030	2022	2020	9	13	1,2,7,9,	
74DI311_2	DS	16088	065	001	ROS/CTD	093006	1318	EN	64 56.10 N	30 37.07 W	GPS	2005					10,20	
74DI311_2	DS	16089	066	001	ROS/CTD	093006	1421	BE	64 50.06 N	30 29.83 W	GPS	2140						LADCP Measurement
74DI311_2	DS	16089	066	001	ROS/CTD	093006	1506	BO	64 50.48 N	30 30.20 W	GPS	2138	2137	2125	13	13	1,2,7,9,	
74DI311_2	DS	16089	066	001	ROS/CTD	093006	1601	EN	64 50.91 N	30 30.64 W	GPS	2123					10,20	
74DI311_2	DS	16090	067	001	ROS/CTD	093006	1940	BE	65 00.05 N	29 15.00 W	GPS	1417						LADCP Measurement
74DI311_2	DS	16090	067	001	ROS/CTD	093006	2022	BO	65 00.71 N	29 15.18 W	GPS	1452	1471	1470	20	5	1,2,7,9,	
74DI311_2	DS	16090	067	001	ROS/CTD	093006	2106	EN	65 00.57 N	29 15.51 W	GPS	1417					10,20	
74DI311_2	DS	16091	068	001	ROS/CTD	093006	2158	BE	65 05.02 N	29 19.90 W	GPS	1669						LADCP Measurement
74DI311_2	DS	16091	068	001	ROS/CTD	093006	2233	BO	65 05.14 N	29 20.15 W	GPS	1711	1720	1700	12	5	1,2,7,9,	
74DI311_2	DS	16091	068	001	ROS/CTD	093006	2315	EN	65 05.34 N	29 20.26 W	GPS	1758					10,20	
74DI311_2	DS	16092	069	001	ROS/CTD	100106	0008	BE	65 09.98 N	29 24.98 W	GPS	1660						LADCP Measurement
74DI311_2	DS	16092	069	001	ROS/CTD	100106	0039	BO	65 10.20 N	29 25.05 W	GPS	1654	1656	1640	7.6	5	1,2,7,9,	
74DI311_2	DS	16092	069	001	ROS/CTD	100106	0115	EN	65 10.60 N	29 25.09 W	GPS	1644					10,20	
74DI311_2	DS	16093	070	001	ROS/CTD	100106	0202	BE	65 14.98 N	29 30.09 W	GPS	1540						LADCP Measurement
74DI311_2	DS	16093	070	001	ROS/CTD	100106	0231	BO	65 15.16 N	29 30.11 W	GPS	1521	1527	1510	11	5	1,2,7,9,	
74DI311_2	DS	16093	070	001	ROS/CTD	100106	0307	EN	65 15.25 N	29 30.27 W	GPS	1532					10,20	
74DI311_2	DS	16094	071	001	ROS/CTD	100106	0351	BE	65 19.91 N	29 34.94 W	GPS	1342						LADCP Measurement
74DI311_2	DS	16094	071	001	ROS/CTD	100106	0424	BO	65 20.02 N	29 34.74 W	GPS	1338	1340	1362	9	6	1,2,7,9,	
74DI311_2	DS	16094	071	001	ROS/CTD	100106	0508	EN	65 19.82 N	29 34.93 W	GPS	1345					10,20	
74DI311_2	DS	16095	072	001	ROS/CTD	100106	0603	BE	65 24.93 N	29 39.92 W	GPS	1050						LADCP Measurement
74DI311_2	DS	16095	072	001	ROS/CTD	100106	0632	BO	65 24.68 N	29 39.79 W	GPS	1065	1061	1070	8	10	1,2,7,9,	
74DI311_2	DS	16095	072	001	ROS/CTD	100106	0712	EN	65 24.15 N	29 39.59 W	GPS	1096					10,20	
74DI311_2	DS	16096	073	001	ROS/CTD	100106	0808	BE	65 29.99 N	29 45.99 W	GPS	665						
74DI311_2	DS	16096	073	001	ROS/CTD	100106	0828	BO	65 29.83 N	29 46.34 W	GPS	658	657	657	2.8	8	1,2,7,9,	
74DI311_2	DS	16096	073	001	ROS/CTD	100106	0855	EN	65 29.62 N	29 47.35 W	GPS	651					10,20	
74DI311_2	DS	16097	074	001	ROS/CTD	100106	0951	BE	65 35.09 N	29 50.10 W	GPS	343						
74DI311_2	DS	16097	074	001	ROS/CTD	100106	1003	BO	65 35.15 N	29 50.34 W	GPS	344	330	330	14.9	3	1,2,7,9,	
74DI311_2	DS	16097	074	001	ROS/CTD	100106	1017	EN	65 35.29 N	29 50.99 W	GPS	332					20	
74DI311_2	DS	16098	075	001	ROS/CTD	100106	1340	BE	65 57.94 N	28 49.92 W	GPS	407						
74DI311_2	DS	16098	075	001	ROS/CTD	100106	1353	BO	65 58.02 N	28 50.23 W	GPS	406	389	390	12	3		

1: Salinity
7: CFC
10: Helium

2: Oxygen
9: Tritium
20: O18

EXPO-CODE	Section Name	Discovery Stat. No.	Stat. No.	Cast No.	Cast Type	Date mmddyy	Time UTC	Code	Position Latitude	Position Longitude	Code	Bottom depth	Max Press.	meter wheel	Bottom Dist.	No. Of Bottles	Param.	Comments
74DI311_2	DS	16098	075	001	ROS/CTD	100106	1405	EN	65 58.09 N	28 50.23 W	GPS	406					1,2	
74DI311_2	DS	16099	076	001	ROS/CTD	100106	1443	BE	65 54.84 N	28 45.10 W	GPS	471						
74DI311_2	DS	16099	076	001	ROS/CTD	100106	1454	BO	65 54.76 N	28 45.23 W	GPS	477	455	451	15	3		
74DI311_2	DS	16099	076	001	ROS/CTD	100106	1459	EN	65 54.70 N	28 45.55 W	GPS	468					1,2	
74DI311_2	DS	16100	077	001	ROS/CTD	100106	1542	BE	65 51.93 N	28 40.13 W	GPS	537						
74DI311_2	DS	16100	077	001	ROS/CTD	100106	1556	BO	65 51.01 N	28 40.70 W	GPS	539	526	520	14	3		
74DI311_2	DS	16100	077	001	ROS/CTD	100106	1612	EN	65 51.65 N	28 41.72 W	GPS	541					1,2	
74DI311_2	DS	16101	078	001	ROS/CTD	100106	1655	BE	65 49.01 N	28 35.49 W	GPS	667						LADCP Measurement
74DI311_2	DS	16101	078	001	ROS/CTD	100106	1713	BO	65 48.90 N	28 36.44 W	GPS	674	655	658	5.3	3		
74DI311_2	DS	16101	078	001	ROS/CTD	100106	1731	EN	65 48.43 N	28 37.38 W	GPS	687					1,2	
74DI311_2	DS	16101	078	002	CTD	100106	1744	BE	65 48.27 N	28 37.81 W	GPS	821.5	860					Microstructure
74DI311_2	DS	16101	078	002	CTD	100106	1823	EN	65 48.01 N	28 38.19 N	GPS							
74DI311_2	DS	16102	079	001	ROS/CTD	100106	1903	BE	65 46.06 N	28 29.90 W	GPS	829						LADCP Measurement
74DI311_2	DS	16102	079	001	ROS/CTD	100106	1928	BO	65 46.11 N	28 29.93 W	GPS	829	813	830	11	3		
74DI311_2	DS	16102	079	001	ROS/CTD	100106	1952	EN	65 46.09 N	28 30.49W	GPS	837					1,2	
74DI311_2	DS	16102	079	002	CTD	100106	1957	BE	65 46.18 N	28 30.52 W	GPS	752.13	777					Microstructure
74DI311_2	DS	16102	079	002	CTD	100106	2043	EN	65 45.76 N	28 30.27 W	GPS							
74DI311_2	DS	16103	080	001	ROS/CTD	100106	2135	BE	65 43.19 N	28 24.90 W	GPS	936	809	800	9	3	1,2	LADCP Measurement
74DI311_2	DS	16103	080	001	ROS/CTD	100106	2200	BO	65 43.44 N	28 24.48 W	GPS	920						
74DI311_2	DS	16103	080	001	ROS/CTD	100106	2226	EN	65 43.77 N	28 24.01 W	GPS	907						
74DI311_2	DS	16103	080	002	CTD	100106	2230	BE	65 43.80 N	28 23.97 N	GPS	821.5	860					Microstructure
74DI311_2	DS	16103	080	002	CTD	100106	2336	EN	65 43.74 N	28 24.25 W	GPS							
74DI311_2	DS	16104	081	001	ROS/CTD	100206	0031	BE	65 40.13 N	28 19.99 W	GPS	1001	1000	990	15.2	3	1,2	LADCP Measurement
74DI311_2	DS	16104	081	001	ROS/CTD	100206	0051	BO	65 40.36 N	28 19.73 W	GPS	1005						
74DI311_2	DS	16104	081	001	ROS/CTD	100206	0115	EN	65 40.63 N	28 19.48 W	GPS	993						
74DI311_2	DS	16104	081	002	CTD	100206	0114	BE	65 40.67 N	28 19.49 W	GPS	920	983					Microstructure
74DI311_2	DS	16104	081	002	CTD	100206	0228	EN	65 40.38 N	28 20.07 W	GPS							
74DI311_2	DS	16105	082	001	ROS/CTD	100206	0313	BE	65 37.06 N	28 15.26 W	GPS	893	881	871	16.5	3	1,2	LADCP Measurement
74DI311_2	DS	16105	082	001	ROS/CTD	100206	0331	BO	65 37.23 N	28 15.56 W	GPS	896						
74DI311_2	DS	16105	082	001	ROS/CTD	100206	0352	EN	65 37.39 N	28 15.68 W	GPS	904						
74DI311_2	DS	16105	082	002	CTD	100206	0410	BE	65 37.36 N	28 37.36 W	GPS	797	877					Microstructure
74DI311_2	DS	16105	082	002	CTD	100206	0455	EN	65 37.29 N	28 15.96 W	GPS							
74DI311_2	DS	16106	083	001	MOR	100206		BE			GPS							Catching for Mooring
74DI311_2	DS	16106	083	001	MOR	100206		EN			GPS							
74DI311_2	DS	16107	084	001	ROS/CTD	100206	1824	BE	66 10.49 N	27 28.94 W	GPS	495	476	470	13.3	3	1,2	
74DI311_2	DS	16107	084	001	ROS/CTD	100206	1838	BO	66 10.41 N	27 28.71 W	GPS	494						

1: Salinity
7: CFC
10: Helium

2: Oxygen
9: Tritium
20: O18

EXPO-	Section	Discovery	Stat.	Cast	Cast	Date	Time		Position			Bottom	Max	meter	Bottom	No. Of	Param.	Comments
CODE	Name	Stat. No.	No.	No.	Type	mmddyy	UTC	Code	Latitude	Longitude	Code	depth	Press.	wheel	Dist.	Bottles		
74DI311_2	DS	16107	084	001	ROS/CTD	100206	1854	EN	66 10.20 N	27 28.21 W	GPS	494						
74DI311_2	DS	16107	084	002	CTD	100206	1904	BE	66 10.03 N	27 21.84 W	GPS	395	406					Microstructure
74DI311_2	DS	16107	084	002	CTD	100206	1932	EN	66 09.29 N	27 26.44 W	GPS							
74DI311_2	DS	16108	085	001	ROS/CTD	100206	2032	BE	66 06.08 N	27 10.19 W	GPS	631	608	604	9	3	1,2	
74DI311_2	DS	16108	085	001	ROS/CTD	100206	2049	BO	66 06.10 N	27 09.96 W	GPS	630						
74DI311_2	DS	16108	085	001	ROS/CTD	100206	2110	EN	66 06.25 N	27 09.77 W	GPS	627						
74DI311_2	DS	16108	085	002	CTD	100206	2104	BE	66 06.23 N	27 09.82 W	GPS							Microstructure, No more data receivedfrom instru
74DI311_2	DS	16108	085	002	CTD	100206					GPS							
74DI311_2	DS	16109	086	001	ROS/CTD	100206	2303	BE	66 02.53 N	26 55.00 W	GPS	583	572	565	11	3	1,2	
74DI311_2	DS	16109	086	001	ROS/CTD	100206	2318	BO	66 02.48 N	26 56.02 W	GPS	586						
74DI311_2	DS	16109	086	001	ROS/CTD	100206	2335	EN	66 02.45 N	26 56.21 W	GPS	586						
74DI311_2	DS	16110	087	001	ROS/CTD	100306	0104	BE	65 59.05 N	27 21.97 W	GPS	654		635	11.6	7		LADCP Measurement
74DI311_2	DS	16110	087	001	ROS/CTD	100306	0122	BO	65 59.06 N	27 21.96 W	GPS	654					1,2 ,7 ,9	
74DI311_2	DS	16110	087	001	ROS/CTD	100306	0142	EN	65 59.05 N	27 21.59 W	GPS	654	639				,20	
74DI311_2	DS	16111	088	001	ROS/CTD	100306	0311	BE	65 54.93 N	27 47.96 W	GPS	627	609	610	14	7		LADCP Measurement
74DI311_2	DS	16111	088	001	ROS/CTD	100306	0341	BO	65 54.76 N	27 48.98 W	GPS	629					1,2 ,7 ,9	
74DI311_2	DS	16111	088	001	ROS/CTD	100306	0401	EN	65 54.74 N	27 48.03 W	GPS	629					,20	
74DI311_2	DS	16112	089	001	ROS/CTD	100306	0524	BE	65 51.96 N	28 12.98 W	GPS	625	601	610	13	8		LADCP Measurement
74DI311_2	DS	16112	089	001	ROS/CTD	100306	0541	BO	65 51.90 N	28 12.78 W	GPS	624					1,2 ,7 ,9	
74DI311_2	DS	16112	089	001	ROS/CTD	100306	0607	EN	65 51.83 N	28 12.68 W	GPS	626					,20	
74DI311_2	DS	16113	090	001	ROS/CTD	100306	0714	BE	65 46.98 N	28 32.26 W	GPS	790	790	795	14	8		O2 only taken from bottle 1,2,3
74DI311_2	DS	16113	090	001	ROS/CTD	100306	0734	BO	65 46.82 N	28 32.12 W	GPS	804					1,2 ,7 ,9	LADCP Measurement
74DI311_2	DS	16113	090	001	ROS/CTD	100306	0804	EN	65 46.46 N	28 32.02 W	GPS	821					,20	
74DI311_2	DS	16114	091	001	ROS/CTD	100306	0933	BE	65 41.98 N	28 56.01 W	GPS	913	900	890	14	3	1,2	Salt and O2 only taken from bottle 1,3,7
74DI311_2	DS	16114	091	001	ROS/CTD	100306	0955	BO	65 41.72 N	28 56.07 W	GPS	917						LADCP Measurement
74DI311_2	DS	16114	091	001	ROS/CTD	100306	1020	EN	65 41.23 N	28 55.74 W	GPS	938						
74DI311_2	DS	16115	092	001	ROS/CTD	100306	1151	BE	65 32.06 N	29 15.03 W	GPS	1047	1049	1035	5	3	1,2	Salt and O2 only taken from bottle 1,3,5
74DI311_2	DS	16115	092	001	ROS/CTD	100306	1215	BO	65 31.69 N	29 15.33 W	GPS	1051						LADCP Measurement
74DI311_2	DS	16115	092	001	ROS/CTD	100306	1241	EN	65 31.53 N	29 15.69 W	GPS	1051						
74DI311_2	DS	16116	093	001	ROS/CTD	100306	1335	BE	65 35.95 N	29 22.17 W	GPS	767	760	760	11	2	1,2	Salt and O2 only taken from bottle 1,2,4
74DI311_2	DS	16116	093	001	ROS/CTD	100306	1354	BO	65 35.75 N	29 22.35 W	GPS	773						LADCP Measurement
74DI311_2	DS	16116	093	001	ROS/CTD	100306		EN			GPS							
74DI311_2	DS	16117	094	001	ROS/CTD	100306	1527	BE	65 28.06 N	29 06.32 W	GPS	1251	1250	1245	3	2	1,2	LADCP Measurement
74DI311_2	DS	16117	094	001	ROS/CTD	100306	1555	BO	65 28.08 N	29 06.36 W	GPS	1250						
74DI311_2	DS	16117	094	001	ROS/CTD	100306	1621	EN	65 27.77 N	29 06.27 W	GPS	1260						
74DI311_2	DS	16118	095	001	ROS/CTD	100306	1759	BE	65 24.03 N	29 39.28 W	GPS	1109	1094	1095	7	1		LADCP Measurement
74DI311_2	DS	16118	095	001	ROS/CTD	100306	1827	BO	65 24.08 N	29 39.74 W	GPS	1099						

1: Salinity
7: CFC
10: Helium

2: Oxygen
9: Tritium
20: O18

EXPO- CODE	Section Name	Discovery Stat. No.	Stat. No.	Cast No.	Cast Type	Date mmddyy	Time UTC	Code	Position Latitude	Position Longitude	Code	Bottom depth	Max Press.	meter wheel	Bottom Dist.	No. Of Bottles	Param.	Comments
74DI311_2	DS	16118	095	001	ROS/CTD	100306	1850	EN	65 24.09 N	29 40.255 W	GPS	1094						
74DI311_2	DS	16119	096	001	ROS/CTD	100306	2024	BE	65 14.95 N	29 59.26 W	GPS	1382	1365	1365	12	0		LADCP Measurement
74DI311_2	DS	16119	096	001	ROS/CTD	100306	2055	BO	65 15.14 N	29 58.98 W	GPS	1378						
74DI311_2	DS	16119	096	001	ROS/CTD	100306	2124	EN	65 14.99 N	29 58.66 W	GPS	1387						
74DI311_2	DS	16119	096	002	CTD	100306	2137	BE	65 14.90 N	29 58.17 W	GPS	1308.5	1394.49					LADCP Measurement
74DI311_2	DS	16119	096	002	CTD	100306	2256	EN	65 13.94 N	29 56.77 W	GPS							
74DI311_2	DS	16120	097	001	ROS/CTD	100406	0038	BE	65 09.95 N	30 28.98 W	GPS	1519	1491	1500	12	0		LADCP Measurement
74DI311_2	DS	16120	097	001	ROS/CTD	100406	0108	BO	65 10.15 N	30 28.62 W	GPS	1510						
74DI311_2	DS	16120	097	001	ROS/CTD	100406	0137	EN	65 10.32 N	30 28.56 W	GPS	1502						
74DI311_2	DS	16121	098	001	ROS/CTD	100406	0313	BE	65 07.05 N	30 55.48 W	GPS	1642	1637	1620	16.8	0		LADCP Measurement
74DI311_2	DS	16121	098	001	ROS/CTD	100406	0350	BO	65 06.99 N	30 55.73 W	GPS	1620						
74DI311_2	DS	16121	098	001	ROS/CTD	100406	0424	EN	65 06.88 N	30 55.81 W	GPS	1653						
74DI311_2	DS	16122	099	001	ROS/CTD	100406	0833	BE	65 27.47 N	32 18.23 W	GPS	823			10	0		LADCP Measurement
74DI311_2	DS	16122	099	001	ROS/CTD	100406	0857	BO	65 27.51 N	32 18.27 W	GPS	816						
74DI311_2	DS	16122	099	001	ROS/CTD	100406	0921	EN	65 27.70 N	32 18.48 W	GPS	789						
74DI311_2	DS	16123	100	001	ROS/CTD	100406	1020	BE	65 22.85 N	32 18.64 W	GPS	1178				0		LADCP Measurement
74DI311_2	DS	16123	100	001	ROS/CTD	100406	1050	BO	65 22.85 N	32 18.63 W	GPS	1179						
74DI311_2	DS	16123	100	001	ROS/CTD	100406	1114	EN	65 22.83 N	32 22.83 W	GPS	1179						
74DI311_2	DS	16124	101	001	ROS/CTD	100406	1221	BE	65 16.69 N	32 12.40 W	GPS	1432	1413	1410	19	0		LADCP Measurement
74DI311_2	DS	16124	101	001	ROS/CTD	100406	1249	BO	65 16.73 N	32 12.21 W	GPS	1435						
74DI311_2	DS	16124	101	001	ROS/CTD	100406	1310	EN	65 16.71 N	32 12.38 W	GPS	1437						
74DI311_2	DS	16125	102	001	ROS/CTD	100406	1456	BE	65 06.82 N	32 03.03 W	GPS	1775	1784	1775	9	0		LADCP Measurement
74DI311_2	DS	16125	102	001	ROS/CTD	100406	1529	BO	65 06.75 N	32 03.54 W	GPS	1784						
74DI311_2	DS	16125	102	001	ROS/CTD	100406	1603	EN	65 06.75 N	32 04.25 W	GPS	1796						

1: Salinity
7: CFC
10: Helium

2: Oxygen
9: Tritium
20: O18